



## OPEN ACCESS

## EDITED BY

Rachel Przeslawski,  
NSW Government, Australia

## REVIEWED BY

Fabrice Stephenson,  
University of Waikato, New Zealand  
Fábio L. Matos,  
University of Aveiro, Portugal

## \*CORRESPONDENCE

Ruiju Tong

[✉ 19821894@fjut.edu.cn](mailto:19821894@fjut.edu.cn)

RECEIVED 06 May 2023

ACCEPTED 11 September 2023

PUBLISHED 13 October 2023

## CITATION

Tong R, Davies AJ, Yesson C, Yu J, Luo Y,  
Zhang L and Burgos JM (2023)  
Environmental drivers and the distribution  
of cold-water corals in the global ocean.  
*Front. Mar. Sci.* 10:1217851.  
doi: 10.3389/fmars.2023.1217851

## COPYRIGHT

© 2023 Tong, Davies, Yesson, Yu, Luo,  
Zhang and Burgos. This is an open-access  
article distributed under the terms of the  
[Creative Commons Attribution License  
\(CC BY\)](https://creativecommons.org/licenses/by/4.0/). The use, distribution or  
reproduction in other forums is permitted,  
provided the original author(s) and the  
copyright owner(s) are credited and that  
the original publication in this journal is  
cited, in accordance with accepted  
academic practice. No use, distribution or  
reproduction is permitted which does not  
comply with these terms.

# Environmental drivers and the distribution of cold-water corals in the global ocean

Ruiju Tong<sup>1,2\*</sup>, Andrew J. Davies<sup>3,4</sup>, Chris Yesson<sup>5</sup>,  
Jinsongdi Yu<sup>6</sup>, Yuan Luo<sup>6</sup>, Ling Zhang<sup>6</sup> and Julian M. Burgos<sup>7</sup>

<sup>1</sup>Department of Transportation, Fujian University of Technology, Fuzhou, China, <sup>2</sup>Institute of Smart Marine and Engineering, Fujian University of Technology, Fuzhou, China, <sup>3</sup>Department of Biological Sciences, University of Rhode Island, Kingston, RI, United States, <sup>4</sup>Graduate School of Oceanography, University of Rhode Island, Narragansett, RI, United States, <sup>5</sup>Institute of Zoology, Zoological Society of London, London, United Kingdom, <sup>6</sup>The Academy of Digital China (Fujian), Fuzhou University, Fuzhou, China, <sup>7</sup>Demersal Division, Marine and Freshwater Research Institute, Hafnarfjörður, Iceland

Species distribution models (SDMs) are useful tools for describing and predicting the distribution of marine species in data-limited environments. Outputs from SDMs have been used to identify areas for spatial management, analyzing trawl closures, quantitatively measuring the risk of bottom trawling, and evaluating protected areas for improving conservation and management. Cold-water corals are globally distributed habitat-forming organisms that are vulnerable to anthropogenic impacts and climate change, but data deficiency remains an ongoing issue for the effective spatial management of these important ecosystem engineers. In this study, we constructed 11 environmental seabed variables at 500 m resolution based on the latest multi-depth global datasets and high-resolution bathymetry. An ensemble species distribution modeling method was used to predict the global habitat suitability for 10 widespread cold-water coral species, namely, 6 Scleractinian framework-forming species and 4 large gorgonian species. Temperature, depth, salinity, terrain ruggedness index, carbonate saturation state, and chlorophyll were the most important factors in determining the global distributions of these species. The Scleractinian *Madrepora oculata* showed the widest niche breadth, while most other species demonstrated somewhat limited niche breadth. The shallowest study species, *Oculina varicosa*, had the most distinctive niche of the group. The model outputs from this study represent the highest-resolution global predictions for these species to date and are valuable in aiding the management, conservation, and continued research into cold-water coral species.

## KEYWORDS

habitat suitability model, cold-water corals, biogeography, ensemble modeling, ecological niche, deep sea, benthic habitats

## 1 Introduction

Cold-water corals are a diverse group of species from various taxonomic groups including stony corals (Order Scleractinia), octocorals (Order Alcyonacea), and hydrocorals (Order Stylasteridae), among others. These species form complex three-dimensional habitats in the deep sea, providing space, refugia, feeding, and nursery grounds for many associated species (Corbera et al., 2019; Price et al., 2021). For example, more than 1,300 species have been found among reefs formed by the Scleractinian coral *Desmophyllum pertusum* [former and now unaccepted synonym *Lophelia pertusa* (Addamo et al., 2016)] in the NE Atlantic (Roberts et al., 2006). Solitary gorgonian octocorals, such as *Paragorgia arborea* and *Primnoa resedaeformis*, also enhance local habitat complexity through their structures and biological interactions, creating three-dimensional biotic habitats both within and between colonies that support invertebrate and fish species (Buhl-Mortensen et al., 2010). These habitats also play a key and emerging role in local nutrient cycling and carbon sequestration processes (de Froe et al., 2019), reflecting their importance as ecosystems that support a range of ecological services in the deep ocean.

The habitats formed by cold-water corals are susceptible to human influences due to their structural fragility and slow growth rate, particularly from bottom trawling and oil drilling (Hall-Spencer et al., 2002; Larsson and Purser, 2011). This sensitivity, combined with their ecological importance, has led to many countries exploring Marine Protected Areas (MPAs) as a means to preserve these habitats (Yesson et al., 2017). However, protection efforts for cold-water corals and many other deep-sea habitats largely remain insufficient and incomplete throughout the world due to a lack of awareness of the distribution of many species (Stephenson et al., 2021b). Species distribution modeling (SDM), also known as habitat suitability modeling or ecological niche modeling, is an increasingly used tool to predict the potential distributions of species based on the premise that environmental factors influence species distributions (Elith et al., 2006; Valavi et al., 2023). They have been used, for example, in determining locations for spatial closure construction (Lagasse et al., 2015; Rowden et al., 2017), the evaluation of trawl closure and the quantitative assessment of bottom trawling (Penney and Guinotte, 2013), the assessment of reserves and protected areas for better protection (Rengstorf et al., 2013; Ross and Howell, 2013; Guinotte and Davies, 2014), the formulation of ecologically and biologically significant areas (EBSAs) (Yesson et al., 2017), and the development of spatial management options that balance the protection of VMEs with the utilization of high value areas for fishing (Rowden et al., 2019), and to estimate the potential effects of oil spills (Georgian et al., 2020).

SDMs have been developed for cold-water corals at a variety of spatial scales, ranging from spatially limited local and regional scales through to broad-scale global models. Local-scale models have largely relied on terrain variables derived from high-resolution locally obtained multibeam bathymetry to draw associations between topography and species distributions (Rowden et al., 2017; Bargain et al., 2018). Regional and basin-scale models have been constructed from broad-scale environmental variables, such as

depth, temperature, and salinity as they are more variable over larger geographical ranges and have been shown to be important drivers of species distribution (Burgos et al., 2020; Matos et al., 2021). Models at the global scale have made use of whole ocean bathymetric data and lower-resolution environmental datasets that have been “upscaled” using approaches that match depth zones with environmental data interpolated at those depths (Davies et al., 2008; Davies and Guinotte, 2011; Yesson et al., 2012; Yesson et al., 2017). However, there remains considerable potential for the improvement of SDMs at large spatial scales, given the limited spatial resolution of environmental variables and the limited geographical range of some key environmental variables (e.g., omega aragonite) of earlier studies. Advancement in techniques for pseudo-absence point selection, modeling approaches, statistics and improvements in computing power will have substantial impact on broad spatial-scale habitat suitability modeling of cold-water corals (Roberts et al., 2017; Sillero and Barbosa, 2021).

Identifying the environmental conditions that shape the distribution of species, exploring how these overlap between related species, and developing understanding of underlying physiological mechanisms are crucial for conservation and resource management in the face of climate change (Aguirre-Gutiérrez et al., 2015). SDM approaches and ordination methods are frequently used to investigate the fundamental ecological niche of species and derive understanding of specific responses to environmental variation (Zhu et al., 2016). These tools can identify the key factors driving species distributions and niche similarities between species, assuming that appropriate environmental variables that have ecological or physiological relevance are incorporated in analyses (Broennimann et al., 2012; Di Cola et al., 2017). However, SDM approaches may confuse niche divergences with geographic distance due to the spatial autocorrelation present in environmental variables (McCormack et al., 2010; Barbosa et al., 2020). The ordination approach principal component analysis (PCA-env) calibrated on the entire environmental space of the study area has been increasingly used to estimate niche overlap in environmental space. As opposed to geographic space, it is independent of sampling effort, thereby offering an important supplement to habitat suitability modeling especially for data-poor species such as cold-water corals (Broennimann et al., 2012; Barbosa et al., 2020).

The cold-water coral species *D. pertusum*, *Madrepora oculata*, *Enallopsammia rostrata*, *Goniocorella dumosa*, *Oculina varicosa*, *Solenosmilia variabilis*, *P. arborea*, *P. resedaeformis*, *Acanella arbuscula*, and *Paramuricea placomus* are widely accepted as indicators of the presence of Vulnerable Marine Ecosystems (VMEs) (Burgos et al., 2020), due to their fragility, slow growth rate, and susceptibility to anthropogenic impacts and climate change. Scleractinian corals *D. pertusum*, *M. oculata*, *E. rostrata*, *G. dumosa*, *O. varicosa*, and *S. variabilis* are all reef-framework forming species with cosmopolitan distributions (Davies and Guinotte, 2011). *Desmophyllum pertusum* often occurs as the dominant framework-forming Scleractinian or as isolated thickets mainly in the North Atlantic (Freiwald et al., 2004; Tong et al., 2016), while *M. oculata* has mainly been found as a secondary framework-forming species within *D. pertusum* or *G. dumosa* reefs

(Freiwald et al., 2004; Roberts et al., 2006). *Goniocorella dumosa* has been observed as the dominant reef-builder in New Zealand waters (Tracey et al., 2011). *Enallopsammia rostrata* is also observed associated with *D. pertusum*, *M. oculata*, and *S. variabilis* (Freiwald et al., 2004). *Oculina varicosa* can inhabit both shallow and deep waters (Reed, 2002). *Paragorgia arborea* and *P. resedaeformis* are among the largest deep-sea gorgonians, which build up tree-like colonies, providing habitats for numerous associated species (Buhl-Mortensen et al., 2005; Tong et al., 2012). The gorgonian species *P. placomus* has been observed mainly within the North Atlantic (Buhl-Mortensen et al., 2015). *Acanella arbuscula* is widespread across both the Atlantic and the Pacific, and is often found in canyon and slope environments (Saucier et al., 2017).

In this study, we aim to improve upon and extend earlier global models of the VME indicator species *D. pertusum*, *M. oculata*, *E. rostrata*, *G. dumosa*, *O. varicosa*, *S. variabilis*, *P. arborea*, *P. resedaeformis*, *A. arbuscula*, and *P. placomus* in the global ocean (Davies et al., 2008; Tittensor et al., 2009; Davies and Guinotte, 2011; Yesson et al., 2012; Yesson et al., 2017; Tong et al., 2022). We follow recently established best practices in SDM (Araújo et al., 2019; Winship et al., 2020) by using gridded bathymetry of the highest resolution available and integrating environmental variables from three data sources with trilinear interpolation to develop new validated seafloor environmental datasets for the global ocean. We use the best available species data within an ensemble modeling framework that incorporates improved statistical techniques such as kernel density estimation (KDE) and block cross-validation approaches to enhance predictive models and subsequent validation. We identify and quantify the environmental variables that shape the ecological niches, estimate ecological niche overlap, and produce high-resolution predictive distribution maps for cold-water corals in the world oceans.

## 2 Methods

### 2.1 Species presences

Presence records of 10 cold-water coral species, *D. pertusum*, *M. oculata*, *E. rostrata*, *G. dumosa*, *O. varicosa*, *S. variabilis*, *P. arborea*, *P. resedaeformis*, *A. arbuscula*, and *P. placomus*, were collected from peer-reviewed manuscripts and online public databases, including OBIS, NOAA Deep-Sea Coral Research and Technology Program, ICES Vulnerable Marine Ecosystems Database, PANGAEA, and the Norwegian MAREANO project. Observations with a reported positional accuracy of  $\leq 500$  m were retained for subsequent predictions, as were the records with no position accuracy information but with directly reported depths within 50 m of the depth inferred from the spatial position following the bathymetric grid used in the study (see below). Fossil-only records of these species were removed. To reduce the impact of sampling bias (i.e., intensity of observations within individual grid cells) on predictions, presence records were further filtered by retaining only a single presence point in each cell of the underlying environmental grid (Boria et al., 2014).

### 2.2 Pseudo-absence points sampling using kernel density estimation

Due to the fact that species location records are gathered more frequently in areas with greater access such as closer to shore and at shallower depths (Ramirez-Llodra et al., 2010), observed distributions often largely reflect sampling effort over the true distribution for the species (Sillero and Barbosa, 2021). For many species in this study, occurrences were mostly obtained from the North Atlantic or in waters around New Zealand due to decades of intensive sampling in these regions (Figure 1). Such sampling bias significantly influences the accuracy of presence-absence SDMs (Winship et al., 2020) and remains largely unaccounted for in global-scale distribution models. In this study, a kernel density estimation (KDE) approach was used that integrates a form of target-group background sampling (Phillips et al., 2009) with random background sampling by selecting randomly placed background points using KDE as probability grid. The KDE was constructed from the filtered presences of all species (only single-species presence retained within each grid cell;  $n = 6,373$  records) (Supplementary Figure 1) and represented the global sampling intensity for the cold-water coral species in this study. A total of 3,069 target-group pseudo-absence points were placed (equal to the largest amount of occurrence records retained of a single species) for each species using the normalized (0–1) KDE as probability grid, excluding any point within a 5-km buffer of any observation records of corresponding species. This approach mirrored the spatial structure of sampling intensity in presence records and has been shown high model performance (Elith et al., 2010; Fitzpatrick et al., 2013; Georgian et al., 2019; Burgos et al., 2020; Georgian et al., 2021).

### 2.3 Environmental variables

The seabed environmental data used in this study were built around a publicly available high-resolution global bathymetric data product obtained from the General Bathymetric Chart of the Ocean. The 2022 grid was assembled from multiple sources, such as acoustic soundings, multibeam bathymetry, and satellite altimetry (GEBCO Compilation Group, 2022). For subsequent variable creation and analysis, the bathymetric grid, originally a 15 arc-second grid, was projected into the NSIDC Equal-Area Scalable Earth (EASE) Grid (EASE-Grid 2.0 Global, EPSG: 6933) with a cell size of 500 m. The projected bathymetric grid was used to calculate seven terrain variables, namely slope, curvature, terrain ruggedness index (TRI), topographic position index (TPI) and roughness using an analysis window size of  $3 \times 3$  cells, and bathymetric position index (BPI) with analysis window sizes of  $3 \times 3$  and  $9 \times 9$  cells (Wilson et al., 2007). Slope, curvature, and BPI were calculated using ArcGIS Pro v2.5. TRI, TPI, and roughness were calculated using QGIS v3.28.2.

Seafloor conditions for 11 variables were obtained via a trilinear interpolation approach whereby each cell of the bathymetric data layer was used to calculate conditions from regularly structured environmental data available at standard depth levels (Table 1).

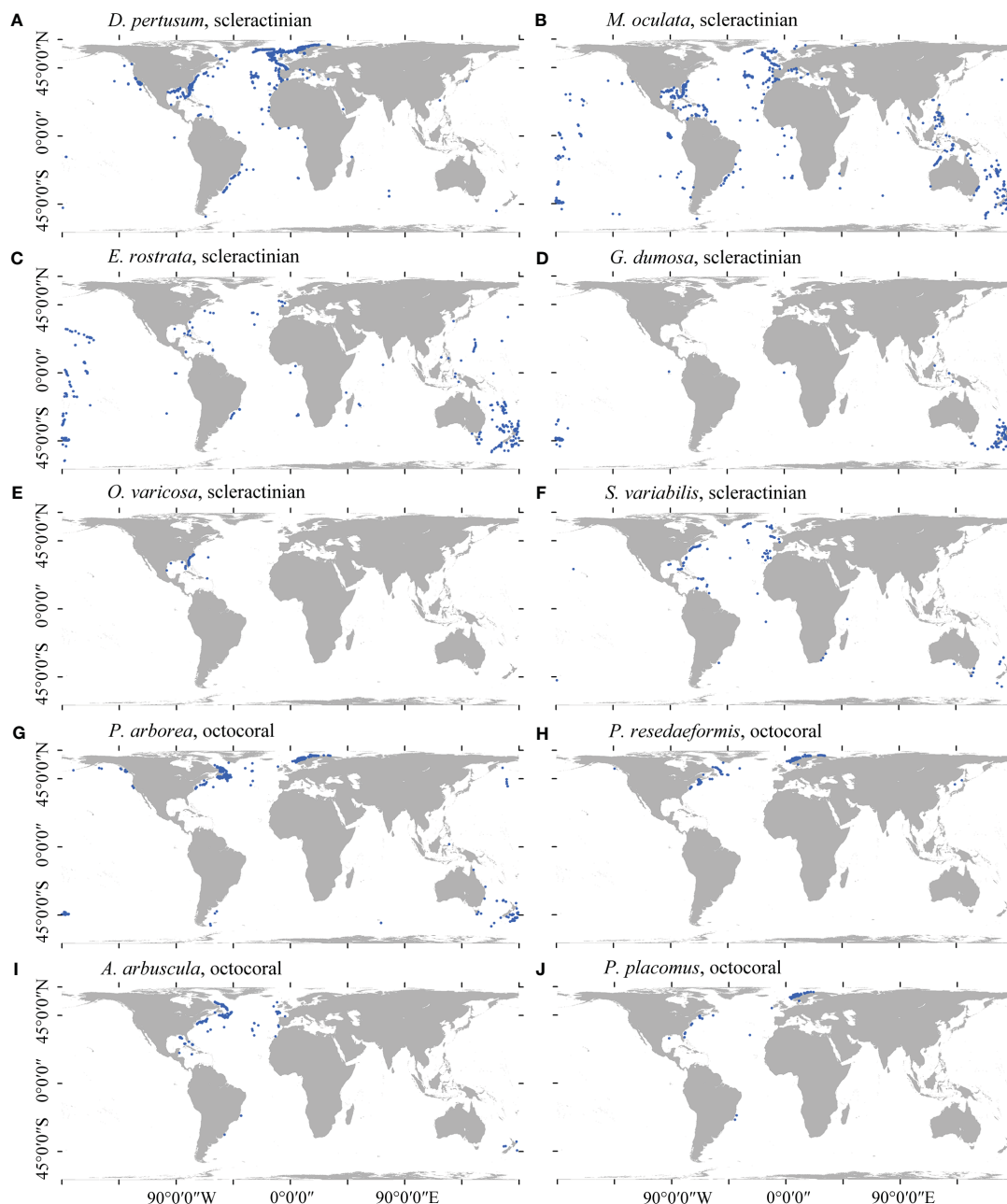


FIGURE 1

Spatial distribution of the cleaned presence records for each of the 10 cold-water coral species in this study. (A) *D. pertusum*, (B) *M. oculata*, (C) *E. rostrata*, (D) *G. dumosa*, (E) *O. varicosa*, (F) *S. variabilis*, (G) *P. arborea*, (H) *P. resedaeformis*, (I) *A. arbuscula*, and (J) *P. placomus*.

Two main inputs were used, World Ocean Atlas 2018 (102 depth layers; mean of all available years for oxygen and nutrient variables, and mean of data collected between 1955 and 2017 for temperature and salinity) (Garcia et al., 2018a; Garcia et al., 2018b; Locarnini et al., 2018; Zweng et al., 2018) and GLODAP V2. 2016b (Global Ocean Data Analysis Project; 33 depth layers; mean of data collected between 1972 and 2013) (Lauvset et al., 2016). Each depth layer was first extracted to a horizontal depth layer of points and resampled to a projected continuous global raster using Natural Neighbor interpolation using the arcpy Python package from ArcGIS Pro v3.1. Where depth cells fell below the

maximum depth of the structured environmental grid, we extrapolated the deepest environmental layer to exceed the maximum depth by 1 m. These layers were then used to create an array of eight points centered around each depth cell from which the environmental condition was estimated using the regular grid interpolator function (trilinear interpolation) from the Python package scipy v1.6.2 (Virtanen et al., 2020). This approach represents improvements over earlier global studies that utilized alternative variable up-scaling approaches (e.g., Davies and Guinotte, 2011), by providing a more accurate interpolation of structured environmental data, and enables an increase in

resolution that is commensurate with the input bathymetric grid (Table 1).

Each interpolated seafloor environmental layer was validated where possible using biogeochemical data obtained from GLODAP, an aggregated and quality controlled water bottle dataset of ocean surface to bottom conditions (Lauvset et al., 2022). Records of bottom values were extracted from GLODAP v2-2022 using Ocean Data View v5.6.3 (Schlitzer, 2023). Estimates of omega aragonite and omega calcite from the GLODAP v2-2022 dataset were calculated from extracted parameter records using the Seacarb algorithm (Gattuso et al., 2022). Linear least squares regression was used to estimate the relationship between the extracted bottle data from GLODAP v2-2022 and the trilinearly interpolated bottom layer for each variable. In addition, a visual spatial validation was conducted by creating a polygon grid with cells sized 500 × 500 km that extended across the model domain (Supplementary Figure 2). Differences between the observed GLODAP data and the predicted trilinear value were expressed as root mean square error (RMSE) on a cell-by-cell basis. For visualization purposes, RMSE was scaled using the standard deviation of all observed GLODAP points for that variable.

Three additional environmental variables of ocean floor conditions were also obtained from two datasets, including the Bio-ORACLE v2.0 dataset (Assis et al., 2018) and Wei (2022) (Table 1), projected to EASE-Grid 2.0 Global and resampled to 500m resolution using bilinear interpolation using Python v3.8 and GDAL v3.2.3. This validation showed significant correlation

between modeled environmental variables and field observations (Pearson's correlation coefficient  $r > 0.93$ ), with the exception of Chlorophyll *a* ( $r = 0.56$ ) obtained from Bio-ORACLE, as reported by Assis et al. (2018). Particulate organic carbon obtained from Wei (2022) was found to be strongly correlated with field observations from a previous study (Lutz et al., 2007) in the North Atlantic with  $r = 0.91$  (Morato et al., 2020).

## 2.4 Correlation analysis of environmental variables

Strongly correlated environmental factors may impede model performance and their ultimate interpretation in SDMs (Huang et al., 2011). In this study, variance inflation factor (VIF) was used to analyze the correlation among environmental variables, with a high VIF value indicating a high degree of co-linearity between a variable and all remaining variables (Yesson et al., 2015; Yesson et al., 2017; Khosravifard et al., 2020). In this study, the VIF was calculated iteratively with the highest VIF variable removed each time, until the VIF value of each retained variable was less than 10, indicating low correlation, using the R package HH v3.1-49 (Heiberger, 2022). Fully automating any procedure to remove highly correlated variables can result in the removal of ecologically relevant factors (Davies and Guinotte, 2011; Yesson et al., 2017; Tong et al., 2022). Therefore, the variables slope, percent oxygen saturation and one of omega aragonite or omega calcite

TABLE 1 Sources and original resolution for environmental variables created in this study.

Environmental variables	Method used	Sources	Resolution
Depth, slope, curvature, BPI3, BPI9, roughness, terrain ruggedness index, topographic position index	Calculated following Wilson et al. (2007)	GEBCO 2022 <sup>1</sup>	15"
Temperature, salinity	Trilinear interpolation, this study	World Ocean Atlas 2018 <sup>2</sup> , GEBCO 2022 <sup>1</sup>	0.25° 15"
Apparent oxygen utilization, dissolved oxygen, percent oxygen saturation, nitrate, phosphate, silicate	Trilinear interpolation, this study	World Ocean Atlas 2018 <sup>2</sup> , GEBCO 2022 <sup>1</sup>	1° 15"
Omega calcite, omega aragonite, pH	Trilinear interpolation, this study	GLODAPV2.2016b <sup>3</sup> , GEBCO 2022 <sup>1</sup>	1° 15"
Chlorophyll at mean depth	Described by Assis et al. (2018)	Bio-ORACLEv2.0 <sup>4</sup> , GEBCO 2015 <sup>5</sup> , PISCES <sup>6</sup>	5', 30", 0.25°
Current velocity at mean depth	Described by Assis et al. (2018)	Bio-ORACLEv2.0 <sup>4</sup> , GEBCO 2015 <sup>5</sup> , ORAP <sup>7</sup>	5', 30", 0.25°
Particulate organic carbon	Wei (2022), described in Morato et al. (2020).	GFDL-ESM2G <sup>8</sup> , IPSL-CM5A-MR <sup>9</sup> , MPI-ESM-MR <sup>10</sup>	0.5° <sup>11</sup>

<sup>1</sup>General Bathymetry Chart of the Oceans 2022 (<https://www.gebco.net/>).

<sup>2</sup>World Ocean Atlas 2018; 102 standard depth layers, temperature and salinity were calculated using 1955–2017 data; oxygen and nutrient variables were calculated using all available data regardless of year of observation.

<sup>3</sup>Global Ocean Data Analysis Project, 33 standard depth layers, calculated using 1972–2013 data.

<sup>4</sup>Bio-ORACLE v2.0, marine data layers for ecological modeling (<https://www.bio-oracle.org/>).

<sup>5</sup>General Bathymetry Chart of the Oceans 2015 (<https://www.gebco.net/>).

<sup>6</sup>Global Ocean Biogeochemistry Non-assimilative Hindcast (resolution: 0.25°/75 vertical levels), monthly averages for the period 2000–2014.

<sup>7</sup>Global Ocean Physics Reanalysis ECMWF (resolution: 0.25°/75 vertical levels), monthly averages for the period 2000–2014.

<sup>8</sup>Geophysical Fluid Dynamics Laboratory's ESM 2G model of CMIP5, yearly means of the period 1951–2000 (historical simulation).

<sup>9</sup>Institut Pierre-Simon Laplace's CM5A-MR model of CMIP5, yearly means of the period 1951–2000 (historical simulation).

<sup>10</sup>Max Planck Institute's ESM-MR model of CMIP5, yearly means of the period 1951–2000 (historical simulation).

<sup>11</sup>Resolution of Wei (2022) is 0.5°. Original resolution for each CMIP5 source was variable, with GFDL-ESM2G 210 rows/360 columns, IPSL-CM5A-MR 149 rows/182 columns and MPI-ESM-MR 404 rows/802 columns.

BPI, bathymetric position index. BPI3 and BPI9 were BPI calculated using window sizes of 3×3 and 9×9, respectively.

dependent upon the skeletal structure of each species were always retained, along with other environmental variables that had VIF <10 (excluding other oxygen parameters were all strongly correlated with Spearman correlation coefficients  $\geq 0.94$ ) (Table 2) (Guinotte et al., 2006a; Sundahl et al., 2020; Matos et al., 2021). Specifically, omega aragonite and omega calcite were used for predictions of Scleractinia and Octocorallia, respectively.

## 2.5 Ensemble species distribution models

Each species distribution modeling method has its own strengths and weaknesses (Liu et al., 2016; Grimmer et al., 2020); ensemble modeling integrates the outputs of multiple species distribution models in a prediction to reduce reliance on a single model or distribution assumption (Robert et al., 2016; Valavi et al., 2022). In this study, we used two machine learning methods, generalized boosting modeling (GBM, also described as boosted regression trees; BRT) (Ridgeway, 1999) and random forests (RF) (Breiman, 2001). GBM employs a boosting algorithm to iteratively call a regression tree algorithm in order to construct a combination of trees (Ridgeway, 1999). GBM iteratively modifies the modeled regression trees to improve their fit to the data (Friedman, 2001) and is often among the best-performing predictive modeling approaches (Elith et al., 2006; Valavi et al., 2022). RF constructs a number of regression trees and then averages them (Breiman, 2001), with the trees growing based on multiple training data subsets that are established via a bagging technique to avoid tree correlation (Rodriguez-Galiano et al., 2015). Both GBM and RF are commonly used for predicting species habitat suitability and often demonstrate high performances when used in ensemble modeling approaches. The R package biomod2 v4.2-1 was used to build the species distribution models (Thuiller et al., 2022).

To generate an individual model for each species, models were run in a block cross-validation approach to reduce the influence of spatial autocorrelation that arises due to geographically concentrated sampling activity (Valavi et al., 2019; Winship et al.,

2020; Valavi et al., 2022). The presence records of each species were evenly divided into five folds based on longitude, with each fold containing one-fifth of the total amount of records, and the pseudo-absence points divided accordingly. For each replicate, four of the five folds were used for model training, with one fold being withheld from model training and used for model validation. AUC [area under the ROC (receiver operator characteristic) curve], TSS (true skill statistic), sensitivity, specificity, and Continuous Boyce Index (Hirzel et al., 2006) were calculated to evaluate the performances of the models.

The ensemble model prediction that combined the GBM and RF models for each species was calculated as the weighted average of each individual model output, utilizing the model performance statistic AUC for each run as weighting and only including predicted models that had an AUC greater than 0.8. The standard deviation of these predicted maps with AUC greater than 0.8 for each species was calculated to provide the information of model uncertainty to support the predictions. Binary habitat suitability maps for each species were calculated using the threshold value calculated from the maximum sensitivity and specificity for each species, setting habitat suitability values below the threshold to zero (unsuitable), and those above to one (suitable). The binary projection for each species was further limited to depth shallower than the maximum depth of the corresponding species' presence. These calculations were performed using ArcGIS Pro v2.5.

## 2.6 Comparison of species' fundamental ecological niches

The ordination method principal component analysis (PCA) was used to investigate the fundamental ecological niches of cold-water coral species. The PCA was calibrated on the entire environmental space of the global ocean (PCA-env) by utilizing values of environmental variables associated with 200,000 randomly selected background points (representing the bottom environmental condition of global ocean) to convert from

TABLE 2 Variable inflation factors (VIF) calculated for each environmental variable, with the variables utilized in predictions highlighted in bold.

Environmental variables	VIF	Environmental variables	VIF
<b>Depth</b>	2.5	<b>Omega aragonite</b>	26.9
<b>Slope</b>	13.9	<b>Omega calcite</b>	5709.9
<b>Curvature</b>	1.9	Dissolved oxygen	3.3
BPI3	$8.3 \times 10^9$	Apparent oxygen utilization	323.8
<b>BPI9</b>	1.9	<b>Percent oxygen saturation</b>	84.7
<b>TRI</b>	1.1	Nitrate	13.7
TPI	58.9	<b>Phosphate</b>	9.2
Roughness	57.1	<b>Silicate</b>	4.8
<b>Temperature</b>	2.9	<b>Chlorophyll</b>	1.9
<b>Salinity</b>	1.2	POC	1.7
<b>pH</b>	6.4	<b>Current velocity</b>	1.1

geographic space to environmental space and create a grid consisting of  $100 \times 100$  pixels (Broennimann et al., 2012; Di Cola et al., 2017). Kernel smoothers were used to quantify densities of species occurrence in the gridded environmental space, delimited by axes with the  $100 \times 100$  pixels, to create an occurrence density grid for each species (Broennimann et al., 2012). Schoener's D metric (Schoener, 1970) was used to estimate niche overlap of species pairs and to test niche similarity and equivalency by determining whether environmental niches of a species pair were more similar than expected by chance, using occurrence density grids of the species pair (Warren et al., 2008; Barbosa et al., 2020). Niche breadth was calculated as the proportion of the available environmental conditions delimited by the axes ( $100 \times 100$  cells) occupied by species in the PCA-env, representing the percentage of available conditions inhabited by the species. The contribution of the environmental variables to the PCA was presented as eigen vectors in the correlation circle plot (Di Cola et al., 2017). The R package Ecospat v3.4 was utilized for the analyses (Broennimann et al., 2022).

### 3 Results

In total, 7,496 presence records, namely, 3,069 for *D. pertusum*, 1,412 for *M. oculata*, 574 for *E. rostrata*, 563 for *G. dumosa*, 148 for *O. varicosa*, 226 for *S. variabilis*, 767 for *P. arborea*, 362 for *P. resedaeformis*, 203 for *A. arbuscula*, and 172 for *P. placomus*, were retained for analyses (Figure 1).

#### 3.1 Validation of environmental variables

Validation of each seafloor environmental variable developed using the trilinear interpolation approach showed significant correlations between the constructed environmental variables and water bottle data ( $R^2$  between 0.786 and 0.987; Figure 2). Spatial validation showed that most variables had low scaled RMSE throughout the global ocean, with higher error values on continental shelf margins where depths change rapidly (Supplementary Figure 2). Temperature and salinity, with higher native horizontal spatial resolutions ( $0.25^\circ$ ), performed better than variables with native resolutions of  $1^\circ$ , although some areas of mid to high RMSE were observed on continental shelves and margins, particularly in the North Atlantic (Supplementary Figure 2). Nevertheless, these variables demonstrated strong correlations with GLODAP data, with  $R^2$  values of 0.930 and 0.877, respectively (Figure 2). Silicate, nitrate, phosphate, apparent oxygen utilization, and dissolved oxygen, with a native horizontal resolution of  $1^\circ$ , showed greater variation in RMSE, but were among the top-ranked variables with strong correlations with GLODAP data (Figure 2 and Supplementary Figure 2). Carbonate variables, omega aragonite and omega calcite, had a larger degree of error, largely in the Atlantic Ocean (Supplementary Figure 2), and performed less well in comparison with GLODAP data in the regression analyses (Figure 2).

#### 3.2 Environmental conditions at species locations

All 10 cold-water coral species were observed predominantly in waters shallower than  $-2,000$  m water depth that had higher mean temperature, pH, and particulate organic carbon than the global means for these variables (Figures 3, 4). In addition, these species were found in areas that were mostly saturated in aragonite and calcite but had a lower mean silicate concentration than the global oceans. *Oculina varicosa* was found in areas that had the greatest differences in environmental conditions compared to the other nine species. On average, *O. varicosa* occurred in much shallower (mean water depth  $-85.2$  m), warmer ( $23.9^\circ\text{C}$ ) and saltier (36.3) waters, with higher means for omega aragonite (saturation state 3.6), percent oxygen saturation (95.3%), pH (8.07), and chlorophyll ( $0.25 \text{ mg/m}^3$ ) compared to other species. Mean phosphate ( $0.19 \text{ }\mu\text{mol/kg}$ ) and mean silicate ( $2.2 \text{ }\mu\text{mol/kg}$ ), in contrast, were lower than mean values for other species locations (Figure 4). *Solenosmilia variabilis* was averagely found in deeper food limited waters that had higher relief and current velocity than other species (mean depth  $-1,190$  m, mean terrain ruggedness index 230.8 m, mean chlorophyll  $0.009 \text{ mg/m}^3$ , and mean current velocity  $0.14 \text{ m/s}$ ). In contrast, *M. oculata* and *E. rostrata* exhibited a more dispersed distribution across broad ranges of depth, temperature, omega aragonite, oxygen saturation, pH, phosphate, and silicate. *Desmophyllum pertusum*, *G. dumosa*, *P. arborea*, *P. resedaeformis*, and *P. placomus* were found predominantly in a relatively narrow range of environmental conditions, especially for depth and silicate (Figures 3, 4). *Acanella arbuscula* was found across a wide depth range ( $-24$  m to  $-4,814$  m, with mean depth  $-1,077$  m) and at the lowest mean temperature  $4.3^\circ\text{C}$ , compared to the other species (Figure 3).

#### 3.3 Variable importance

The strongest contributors, assessed by the mean variable importance score from the fivefold block cross-validation predictions for each species, were largely temperature and depth, but salinity was also observed to be a strong contributor for several species followed by variables such as TRI, chlorophyll, carbonate saturation state, current velocity, and oxygen saturation (Table 3). For 5 of the 10 species, the two modeling approaches agreed as to the top contributing variables, but some differences in the top three variables selected were present (Table 3). Temperature, salinity, and TRI were most important in predictions for *D. pertusum*, while depth, temperature, and percent oxygen saturation were most important in predictions for *M. oculata*, as well as depth, salinity, and TRI for *E. rostrata*, depth, chlorophyll, and temperature for *P. arborea* and *P. resedaeformis*, and depth, TRI, and temperature for *P. placomus*. TRI and temperature were most important in predictions for *S. variabilis*, while salinity and temperature were most important in predictions for *G. dumosa*, as well as salinity, chlorophyll, and current velocity to *O. varicosa*, and omega calcite, salinity, and temperature to *A. arbuscula* (Table 3).

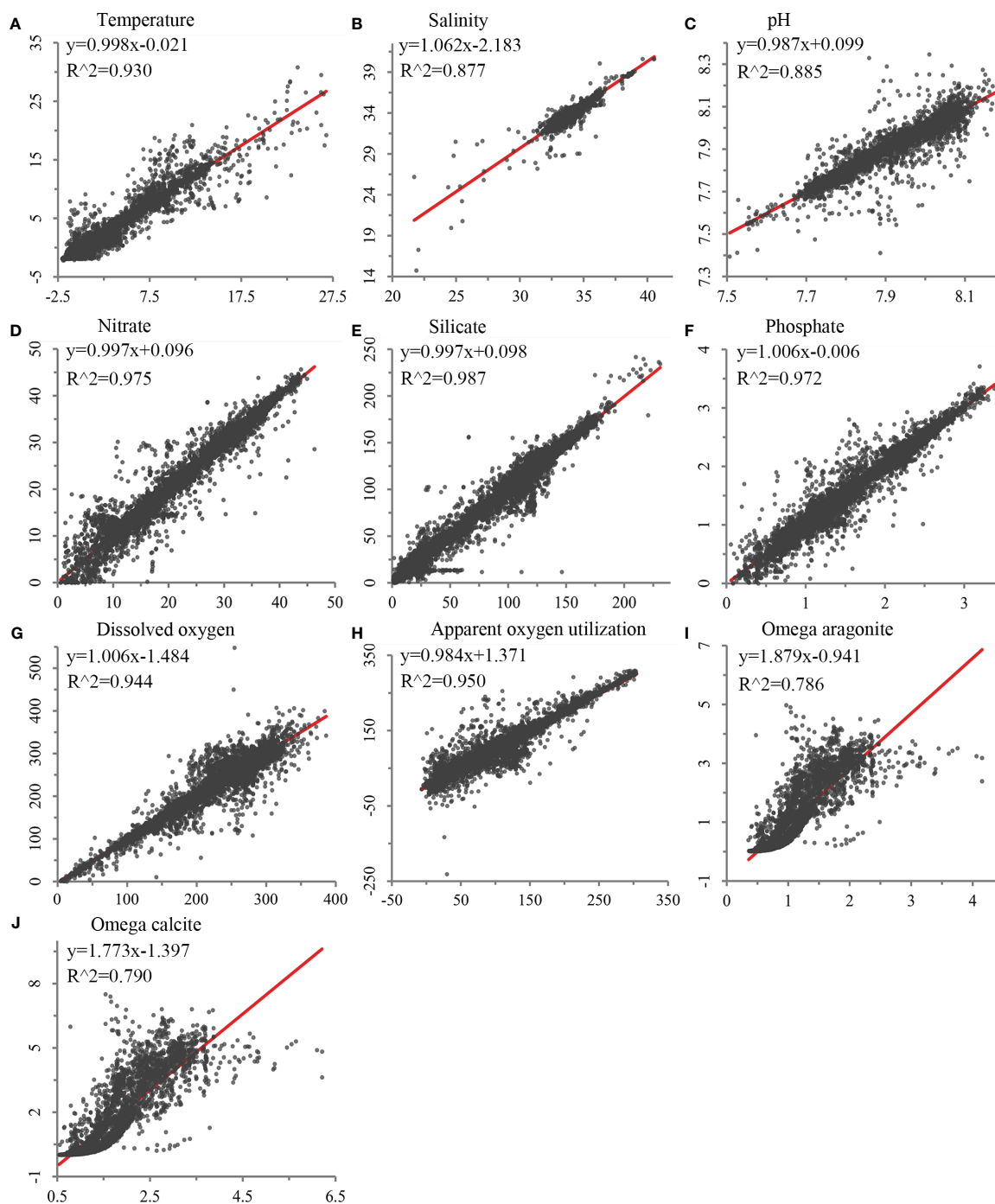


FIGURE 2

Validation of environmental variables built in this study against field sampling data using least squares regression, using bottle data for (A) temperature ( $N = 27,983$ ), (B) salinity ( $N = 27,556$ ), (C) pH ( $N = 9,559$ ), (D) nitrate ( $N = 21,453$ ), (E) silicate ( $N = 21,799$ ), (F) phosphate ( $N = 20,158$ ), (G) dissolved oxygen ( $N = 24,782$ ), (H) apparent oxygen utilization ( $N = 24,123$ ), and (I) omega aragonite and (J) omega calcite ( $N = 9,559$ ).

### 3.4 Model performance and predicted habitat suitability

In this study, both the GBM and RF approaches performed well, with mean AUC values for GBM predictions ranging from 0.871 to 0.984 (standard deviation: 0.015 to 0.115). Similarly, RF models performed well with mean AUC values of 0.87 to 0.993 (standard deviation: 0.007 to 0.115) for all species (Table 4). The mean TSS

value for each species greater than 0.655 showed good agreement between predicted habitat suitability and the known presence/pseudo-absence of the validation dataset. The mean sensitivity was greater than the corresponding mean specificity for most species, including 7 out of 10 species in GBM predictions and 6 out of 10 species in RF predictions, indicating that the models had a higher ability to correctly identify the presence of suitable habitat compared to the pseudo-absence points. The Continuous Boyce

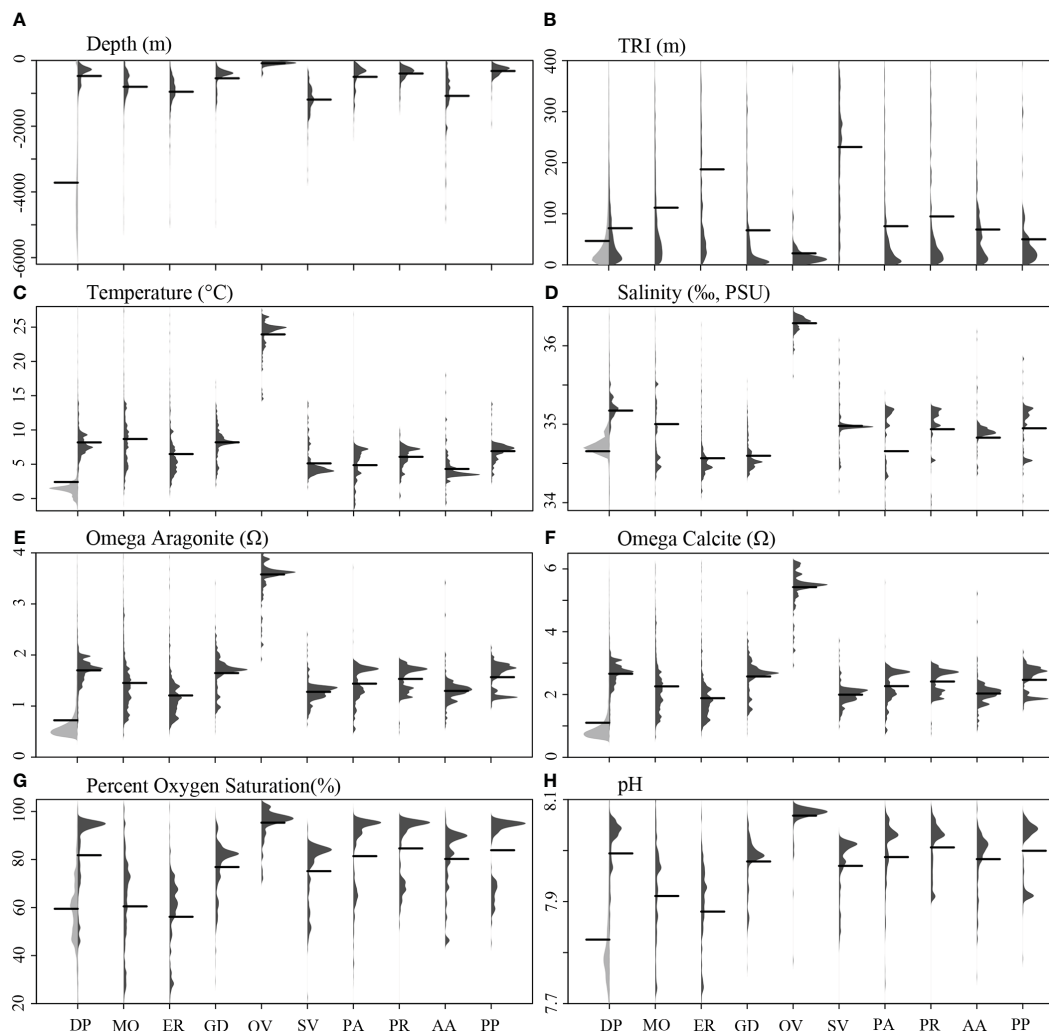


FIGURE 3

The distribution profiles of eight environmental variables are shown for each of the 10 cold-water coral species (shown in dark gray) in contrast to the global background (shown in light gray in the first column of each panel). The environmental variables examined include (A) depth, (B) TRI, (C) temperature, (D) salinity, (E) omega aragonite, (F) omega calcite, (G) percent oxygen saturation, and (H) pH. Black lines represent mean values. Species names were abbreviated for clarity: DP, *D. pertusum*; MO, *M. oculata*; ER, *E. rostrata*; GD, *G. dumosa*; OV, *O. varicosa*; SV, *S. variabilis*; PA, *P. arborea*; PR, *P. resedaeformis*; AA, *A. arbuscula*; and PP, *P. placomus*.

Index of these model runs was variable, but with the mean value  $\geq 0.616$  suggesting a positive correlation between the model's predictions and the observed presences (Table 4). Predicted habitat suitability for each cold-water coral species varied substantially by geographic region around the world (Figures 5–8), with the most suitable habitat found on continental shelves and margins in the North Atlantic, West and South Pacific, the Gulf of Mexico, the Caribbean Sea, the Mediterranean Sea, the Red Sea, and the seamounts and steep slopes of oceanic islands.

Several specific regional differences were observed for each species. *Desmophyllum pertusum*, for example, was predicted predominantly in the NE Atlantic, around the Mediterranean Sea, and on the continental margin off the SE USA (Figure 5A and Supplementary Figure 3A). In comparison, the predicted suitable habitat for *M. oculata* and *E. rostrata* was less prevalent in the North Atlantic and more so in the West and South Pacific and the Red Sea, around the Mediterranean Sea, the Gulf of Mexico, and the Caribbean Sea (Figures 5B, C and

Supplementary Figures 3B, C). The predicted habitat suitability for each species differed substantially in terms of areal extent, with *M. oculata* having the greatest potential range and *O. varicosa* having the smallest, being largely restricted to some areas off the SE USA and regions off South America (Figures 5B, 6B and Supplementary Figures 3B, 4B). Suitable habitat for *G. dumosa* was predicted in the West and South Pacific, particularly in the waters surrounding New Zealand, as well as along the continental margin off SW Africa (Figure 6A and Supplementary Figure 4A). *Solenosmilia variabilis* was predicted predominantly in the North Atlantic, around the Caribbean Sea and the Gulf of Mexico, particularly along the Mid-Atlantic Ridge, as well as in the South Pacific (Figure 6C and Supplementary Figure 4C). The majority of suitable habitat for *P. arborea* was found on the continental shelves of the North Atlantic and the North Pacific, off the southeastern coast of South America, southeastern New Zealand, and on seamounts (Figure 7A and Supplementary Figure 5A). In contrast to *P. arborea*, *P.*

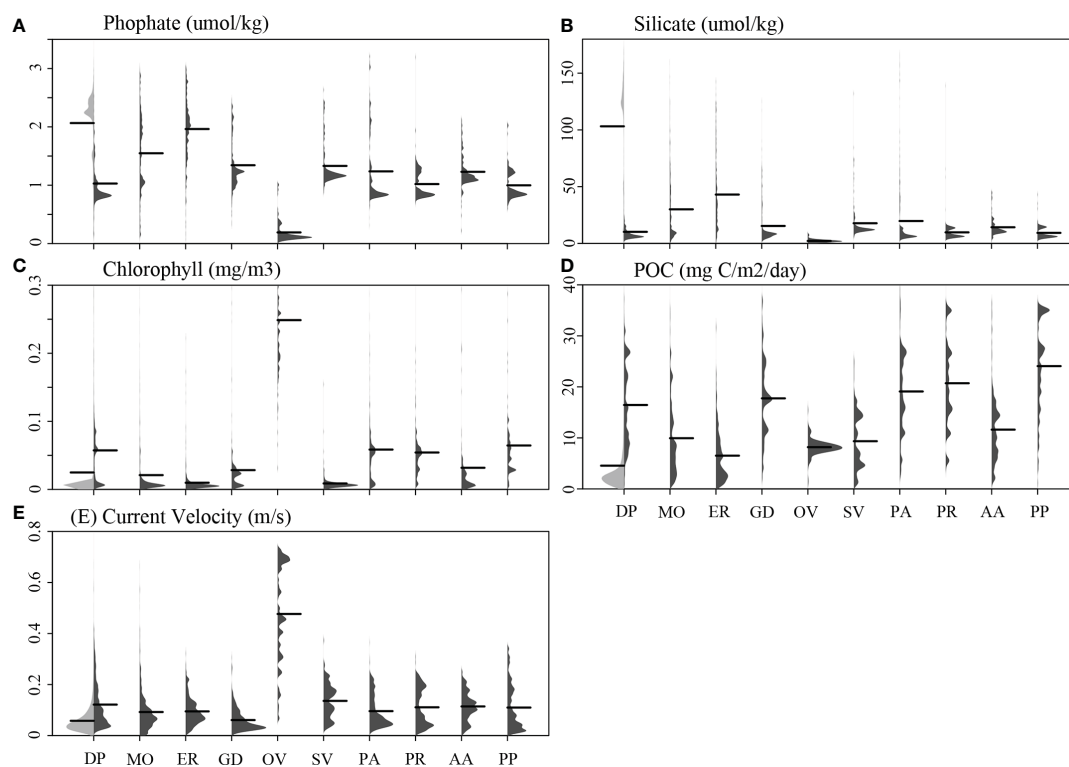


FIGURE 4

The distribution profiles of five environmental variables are shown for each of the 10 cold-water coral species (shown in dark gray) in contrast to the global background (shown in light gray in the first column of each panel). The environmental variables examined include (A) phosphate, (B) silicate, (C) chlorophyll, (D) POC, and (E) current velocity. Black lines represent mean values. Species names were abbreviated for clarity: DP, *D. pertusum*; MO, *M. oculata*; ER, *E. rostrata*; GD, *G. dumosa*; OV, *O. varicosa*; SV, *S. variabilis*; PA, *P. arborea*; PR, *P. resedaeformis*; AA, *A. arbuscula*; PP, *P. placomus*.

*resedaeformis* and *P. placomus* were predicted to have a more restricted suitable habitat, mainly in the North Atlantic (Figures 7B, 8B and Supplementary Figures 5B, 6B). *Acanella arbuscula* was predicted to occur predominantly on the continental shelf margin of the West Atlantic (Figure 8A and Supplementary Figure 6A). The standard deviation of predicted maps for each species showed more areas of higher uncertainty for *G. dumosa* predictions than those for other species (Supplementary Figure 7).

### 3.5 Ecological niche comparison

Among the environmental variables utilized in predictions, the terrain variables slope, curvature, and BPI rarely were important in predictions for the 10 species and, therefore, were excluded from further ecological niche analysis. Twelve environmental variables (depth, TRI, temperature, salinity, pH, omega aragonite, phosphate, silicate, percent oxygen saturation, chlorophyll, particulate organic carbon, and current velocity) were used in the ecological niche analysis for each species (Figure 9).

The correlation circle of PCA-env describes the contribution of each variable to the global environmental conditions captured by the first two principal components, which can help to further identify and understand the environmental variables that shape ecological niches. It shows that omega aragonite, pH, and

temperature mainly contribute to the first principal component axis (PC1), and salinity and TRI mainly contribute to the second principal component axis (PC2), while depth, percent oxygen saturation, current velocity, chlorophyll, particulate organic carbon, phosphate and silicate contribute to both PC1 and PC2 axes (Figure 9M). The two principal components explained 46.46% and 11.94% of the information regarding the global environmental conditions, respectively (Figure 9M). The ecological niche breadth of each species significantly varied, with *M. oculata* having the broadest niche, followed by *E. rostrata* (Figures 9B, C). The location of niche density center of *O. varicosa* was quite different to niche density centers of nine other species, with limited overlap (Figure 9E; Table 5). The niche density centers of *S. variabilis* and *A. arbuscula* were close, with their niches showing high level of overlap (Figures 9F, I). The niche density centers of *D. pertusum*, *G. dumosa*, *P. arborea*, *P. resedaeformis*, and *P. placomus* were close, showing high level degree of niche overlap between each pair of these species, particularly for *P. resedaeformis* and *D. pertusum*, and *P. resedaeformis* and *P. placomus* (Figures 9A, D, G, H, J; Table 5). The niche similarity for each pair of species was all rejected with  $p > 0.05$ , except between *D. pertusum* and *P. resedaeformis*, between *D. pertusum* and *P. placomus*, and between *P. resedaeformis* and *P. placomus*. There were certain degree of niche overlap between Scleractinia and Octocorallia (Figures 9K, L; Table 5). No evidence of niche equivalency was found (Table 5).

TABLE 3 Mean variable importance of each environmental variable in models constructed using fivefold block cross-validation, with the top three highest scoring variables highlighted in bold for each model and species combination.

	<i>D. pertusum</i>		<i>M. oculata</i>		<i>E. rostrata</i>		<i>G. dumosa</i>		<i>O. varicosa</i>		<i>S. variabilis</i>		<i>P. arborea</i>		<i>P. resedaeformis</i>		<i>A. arbuscula</i>		<i>P. placomus</i>	
	GBM	RF	GBM	RF	GBM	RF	GBM	RF	GBM	RF	GBM	RF	GBM	RF	GBM	RF	GBM	RF	GBM	RF
Depth	0.040	0.060	<b>0.153</b>	<b>0.091</b>	<b>0.251</b>	<b>0.065</b>	<b>0.025</b>	0.033	0.000	0.006	0.015	0.019	<b>0.294</b>	<b>0.054</b>	<b>0.224</b>	<b>0.062</b>	0.010	0.031	<b>0.595</b>	<b>0.079</b>
Temperature	<b>0.164</b>	<b>0.076</b>	<b>0.177</b>	<b>0.103</b>	0.017	0.030	<b>0.508</b>	<b>0.088</b>	0.002	0.013	<b>0.163</b>	<b>0.028</b>	<b>0.101</b>	0.043	<b>0.080</b>	0.025	<b>0.073</b>	<b>0.052</b>	<b>0.113</b>	0.018
Salinity	<b>0.081</b>	<b>0.146</b>	0.003	0.015	0.093	<b>0.088</b>	<b>0.438</b>	<b>0.093</b>	<b>0.556</b>	<b>0.018</b>	0.002	0.016	0.030	<b>0.053</b>	0.025	0.014	<b>0.109</b>	0.038	0.017	0.008
TRI	<b>0.120</b>	0.043	0.119	0.047	<b>0.109</b>	<b>0.034</b>	0.007	0.015	0.002	0.006	<b>0.507</b>	<b>0.092</b>	0.031	0.024	0.078	0.028	0.004	0.011	<b>0.091</b>	<b>0.057</b>
Omega calcite													0.040	0.035	0.056	<b>0.030</b>	<b>0.204</b>	<b>0.073</b>	0.036	0.027
Omega aragonite	0.019	<b>0.063</b>	0.002	0.017	0.001	0.015	0.005	<b>0.047</b>	0.000	0.012	0.007	0.026								
Chlorophyll	0.001	0.010	0.007	0.030	0.006	0.017	0.001	0.015	<b>0.431</b>	<b>0.014</b>	0.002	0.010	<b>0.202</b>	<b>0.093</b>	<b>0.176</b>	<b>0.053</b>	0.033	0.020	0.020	0.027
POXS	0.001	0.012	<b>0.135</b>	<b>0.063</b>	<b>0.102</b>	0.027	0.007	0.015	0.002	0.002	0.004	0.006	0.003	0.033	0.000	0.026	0.006	0.033	0.008	0.022
Current velocity	0.004	0.013	0.001	0.006	0.001	0.005	0.000	0.004	<b>0.067</b>	<b>0.063</b>	0.017	0.014	0.002	0.009	0.001	0.013	0.043	<b>0.056</b>	0.009	0.027
Slope	0.000	0.013	0.001	0.018	0.003	0.018	0.001	0.007	0.000	0.004	0.002	<b>0.033</b>	0.001	0.009	0.001	0.016	0.002	0.008	0.000	0.019
Phosphate	0.005	0.014	0.001	0.009	0.003	0.023	0.006	0.034	0.000	0.004	<b>0.022</b>	0.017	0.004	0.016	0.052	0.011	0.044	0.040	0.008	0.012
POC	0.009	0.018	0.004	0.014	0.015	0.023	0.004	0.014	0.024	0.004	0.002	0.006	0.007	0.029	0.014	0.026	0.013	0.022	0.003	<b>0.036</b>
Curvature	0.000	0.002	0.000	0.004	0.000	0.004	0.000	0.002	0.000	0.001	0.000	0.019	0.000	0.004	0.000	0.011	0.001	0.002	0.000	0.008
BPI9	0.001	0.005	0.008	0.013	0.008	0.021	0.003	0.008	0.000	0.002	0.002	0.016	0.002	0.009	0.000	0.010	0.001	0.003	0.010	0.029
pH	0.001	0.013	0.000	0.015	0.000	0.010	0.002	0.011	0.001	0.004	0.003	0.006	0.004	0.014	0.007	0.011	0.003	0.051	0.023	0.017
Silicate	0.001	0.013	0.003	0.013	0.002	0.013	0.005	0.026	0.001	0.010	0.008	0.014	0.001	0.010	0.001	0.010	0.041	0.032	0.001	0.009

POXS, percent oxygen saturation; BPI, bathymetric position index; POC, particulate organic carbon.

TABLE 4 Model evaluation results, including mean and standard deviation of AUC, TSS, sensitivity, specificity and Continuous Boyce Index values from the fivefold block cross-validation of predictions for each individual species using the two modeling approaches, GBM and RF.

	AUC		TSS		Sensitivity		Specificity		Continuous Boyce Index	
	GBM	RF	GBM	RF	GBM	RF	GBM	RF	GBM	RF
<i>D. pertusum</i>	0.924 ± 0.015	0.93 ± 0.014	0.723 ± 0.065	0.737 ± 0.056	0.873 ± 0.049	0.922 ± 0.03	0.853 ± 0.028	0.816 ± 0.075	0.908 ± 0.05	0.976 ± 0.023
<i>M. oculata</i>	0.927 ± 0.023	0.928 ± 0.024	0.743 ± 0.054	0.751 ± 0.062	0.879 ± 0.039	0.896 ± 0.025	0.866 ± 0.038	0.856 ± 0.061	0.942 ± 0.019	0.948 ± 0.069
<i>E. rostrata</i>	0.941 ± 0.033	0.946 ± 0.033	0.796 ± 0.079	0.814 ± 0.073	0.915 ± 0.031	0.937 ± 0.03	0.883 ± 0.074	0.878 ± 0.057	0.843 ± 0.118	0.931 ± 0.062
<i>G. dumosa</i>	0.892 ± 0.071	0.89 ± 0.087	0.724 ± 0.164	0.708 ± 0.206	0.94 ± 0.043	0.851 ± 0.23	0.786 ± 0.127	0.857 ± 0.088	0.822 ± 0.038	0.798 ± 0.081
<i>O. varicosa</i>	0.984 ± 0.021	0.993 ± 0.007	0.928 ± 0.075	0.952 ± 0.052	0.96 ± 0.072	0.993 ± 0.015	0.969 ± 0.053	0.966 ± 0.053	0.863 ± 0.127	0.778 ± 0.213
<i>S. variabilis</i>	0.958 ± 0.039	0.956 ± 0.054	0.852 ± 0.103	0.833 ± 0.151	0.943 ± 0.059	0.908 ± 0.089	0.911 ± 0.064	0.928 ± 0.063	0.881 ± 0.097	0.864 ± 0.102
<i>P. arborea</i>	0.871 ± 0.055	0.892 ± 0.037	0.655 ± 0.141	0.692 ± 0.107	0.915 ± 0.111	0.874 ± 0.1	0.742 ± 0.116	0.821 ± 0.085	0.616 ± 0.397	0.696 ± 0.237
<i>P. resedaeformis</i>	0.922 ± 0.057	0.938 ± 0.038	0.759 ± 0.155	0.774 ± 0.13	0.958 ± 0.041	0.942 ± 0.063	0.802 ± 0.121	0.833 ± 0.099	0.628 ± 0.242	0.886 ± 0.1
<i>A. arbuscula</i>	0.871 ± 0.115	0.87 ± 0.115	0.671 ± 0.196	0.682 ± 0.189	0.789 ± 0.238	0.785 ± 0.24	0.884 ± 0.087	0.899 ± 0.096	0.716 ± 0.234	0.693 ± 0.187
<i>P. placomus</i>	0.927 ± 0.037	0.932 ± 0.039	0.758 ± 0.066	0.763 ± 0.072	0.866 ± 0.106	0.883 ± 0.096	0.894 ± 0.058	0.884 ± 0.046	0.704 ± 0.23	0.753 ± 0.159

## 4 Discussion

In this study, using a high-resolution bathymetric grid, updated environmental variables, and presence records, new predictions of the global distribution of 10 cold-water coral species are developed and have reached a high level of resolution, allowing for additional analyses into the species niches of these enigmatic cold-water coral habitats.

### 4.1 Improvements over earlier studies

The current study represents a substantial improvement in the resolution and geographic extent of distribution predictions for cold-water corals in the deep ocean (Davies and Guinotte, 2011; Yesson et al., 2012; Yesson et al., 2017; Tong et al., 2022). The resolution of the bathymetric dataset is now approximately 500 m (compared with the previous ~1 km), while coverage of high-quality acoustic measurements now covers 24.7% of the global seafloor (calculated using the GEBCO Type Identifier Grid) (Supplementary Figure 8) (GEBCO Compilation Group, 2022). These high-quality measurements were predominantly located in the North Atlantic and in areas of the East, West, and South Pacific, particularly surrounding the continental margins and large oceanic islands, generally consistent with currently known locations of cold-water corals (Supplementary Figure 8; Figure 1). However, the majority of the bathymetry layer was generated from indirect methods that are characterized by low resolution, such as satellite-derived gravity

measurements. These data are further interpolated and lead to the generation of a relatively smooth surface that largely misses a number of seafloor features such as seamounts and canyons below a certain size (Kvile et al., 2014; Yesson et al., 2021). Given that depth remains a critically important variable in assessing global cold-water coral distribution, and that terrain variables such as TRI have emerged as increasingly important in global-scale models, ongoing efforts to improve global bathymetric data will continue to enhance distribution models generated at regional to global scales. GEBCO's Seabed 2030 project is one such initiative, which aims for complete global coverage by 2030, and will serve to improve our ability to predict species distributions (Mayer et al., 2018; Wolff et al., 2019), particularly those in under-surveyed environments.

The quality of the underlying environment layers has also improved since the earlier studies, as evidenced by the higher regression  $R^2$  values for five out of six variables built in this study compared to the validation results of the six variables in the widely used Bio-ORACLE v2.0 dataset, including salinity, nitrate, phosphate, silicate, and dissolved oxygen, only with the exception of temperature (Assis et al., 2018). Previous studies used inverse distance weighting interpolation and a resampling methodology utilizing a bathymetric grid to downscale global environmental variables obtained from NOAA's World Ocean Atlas (Boyer et al., 2005; Garcia et al., 2006a; Garcia et al., 2006b), which was available at a source horizontal resolution of 0.25° for temperature and salinity, and 1° for other variables (Davies and Guinotte, 2011; Yesson et al., 2017). Vertical resolution has been significantly extended, increasing from the 33 World Ocean Atlas depth layers

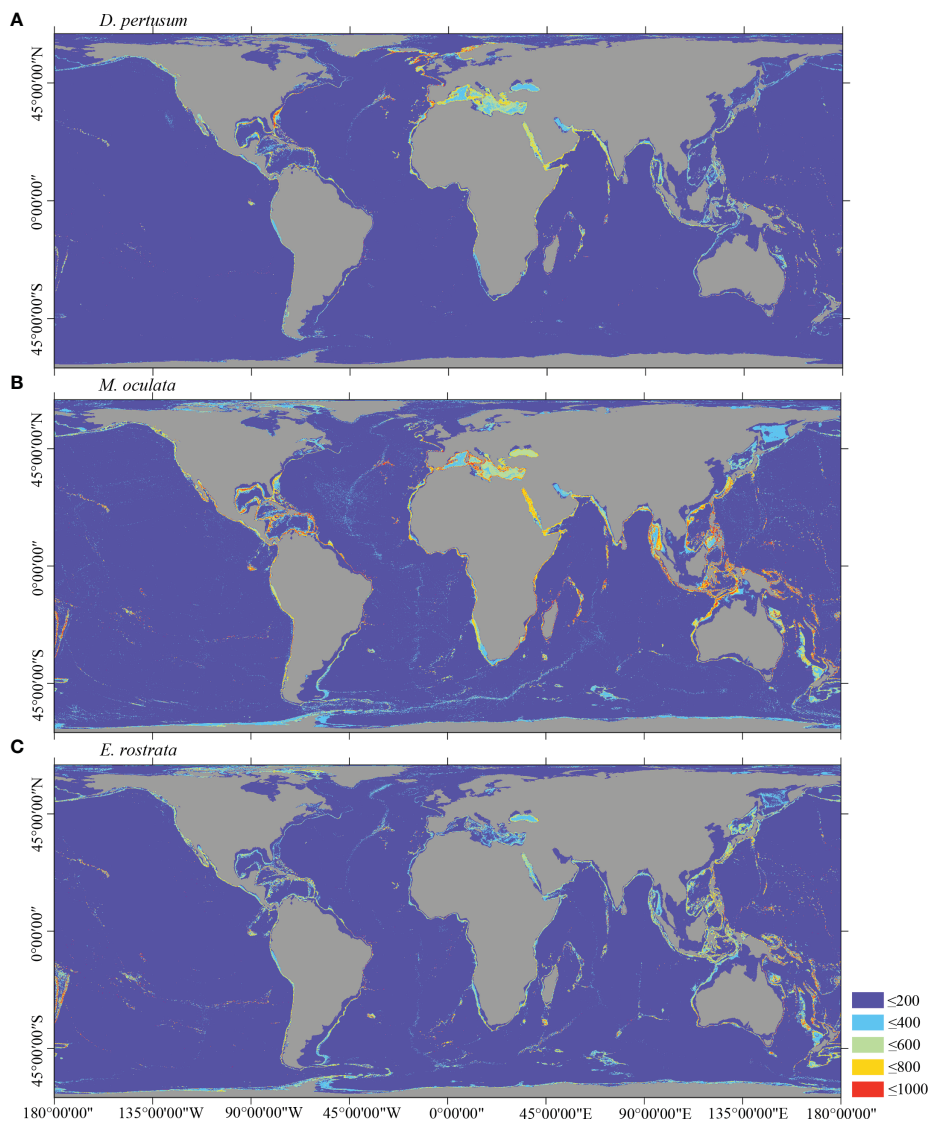


FIGURE 5

Predicted habitat suitability (0–1,000) at the global scale for cold-water corals (A) *D. pertusum*, (B) *M. oculata*, and (C) *E. rostrata* using ensemble modeling. Warmer color shows areas of high habitat suitability.

used in Davies and Guinotte (2011) to the 102 depth layers that are used in this study (Garcia et al., 2018a; Garcia et al., 2018b; Locarnini et al., 2018). The increase in vertical resolution and the use of a new interpolation technique (trilinear interpolation) provide a substantial improvement in the estimations of seafloor condition, particularly in depths shallower than or equal to 2,000 m, where the majority of coral species are found, and lead to finer and more constrained predictions (Figure 10).

The species pool in this study was widened by adding four common gorgonians, which have not been modeled in a consistent fashion before in a global study, enabling global assessment of the niche of cold-water coral species. The number of presence records for most species used in this study was significantly larger than in previous global modeling studies for cold-water corals (Davies and Guinotte, 2011). Compared to earlier studies, these data represent an increase in data density for most species, including a minimum

of 356% (*D. pertusum*), 239% (*M. oculata*), 267% (*E. rostrata*), and 245% (*G. dumosa*), while *S. variabilis* has decreased to 59% of its earlier quantity (Davies et al., 2008; Davies and Guinotte, 2011). The improved grid cell size of 500 m also played a role in increasing the total number of presence records used in predictions as it allowed for the retention of a single record within a grid cell. However, strict limitations of positional and depth accuracy (500 m horizontal or 50 m vertical) were used to constrain to a subset of high-quality presences that have additional metadata, excluding a number of presence records that were utilized in earlier studies (Davies and Guinotte, 2011). The significant increase of presences can improve the model performances (Grimmett et al., 2020), but particular attention should be focused on increasing the taxonomic quality, accuracy, and delivery of metadata to further ensure that modeling efforts in the deep ocean are valid and reach sufficient standards as outlined by Araújo et al. (2019).

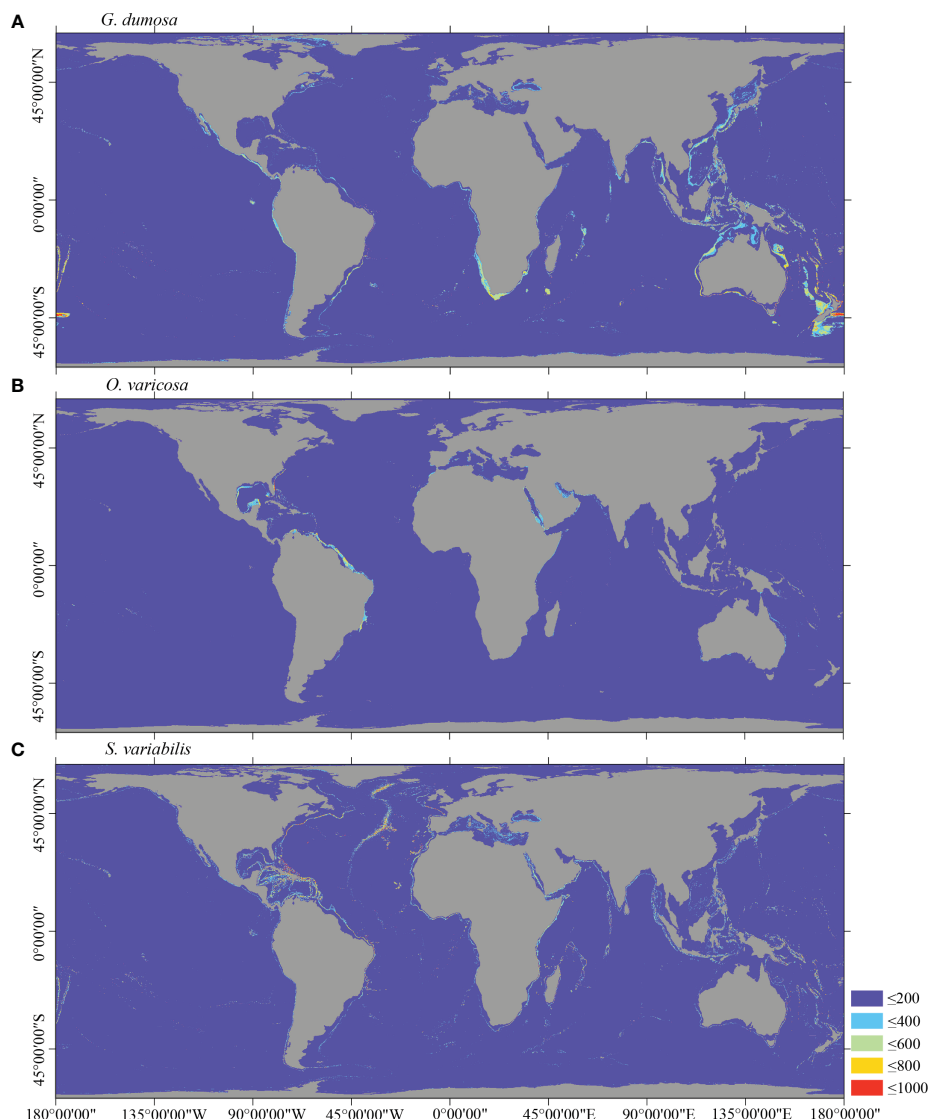


FIGURE 6

Predicted habitat suitability (0–1,000) at the global scale for cold-water corals (A) *G. dumosa*, (B) *O. varicosa*, and (C) *S. variabilis* using ensemble modeling. Warmer colors show areas of high habitat suitability.

Comparing our models with large-scale predictions, it is evident that our models have significantly improved compared to previous efforts (e.g., Figure 10). This improvement can be attributed partly to the inclusion of environmental variables of higher horizontal and vertical resolution in our models than previous studies (Connor et al., 2018). Nevertheless, it is important to note that despite these advancements, our models still tend to over-predict when compared to predictions at the local and sub-regional scale that use additional high-resolution environmental variables. For example, extensive suitable habitat for *D. pertusum*, *P. arborea*, and *P. resedaeformis* predicted on the Norwegian margin was broadly similar to previous high-resolution regional prediction, but over-predicted compared to models incorporating seafloor substratum and marine landscape metrics (Sundahl et al., 2020). In the Mediterranean Sea, high suitable habitat for *D. pertusum* was predicted predominantly along the upper slope and submarine canyons of the Western and Central margins, which is consistent

with the findings of Matos et al. (2021). However, there is still an issue of over-prediction, particularly in the northeast section of the Mediterranean Sea. Similarly, in New Zealand waters, the pattern of significantly higher predicted habitat suitability on Chatham Rise compared to Campbell Plateau for *G. dumosa* aligns with the regional prediction that incorporates higher-resolution environmental variables, such as tidal current speed at a resolution of 1 km (Stephenson et al., 2021a). Nonetheless, over-prediction remains a concern. Habitat suitability models built at smaller spatial scales likely provide more accurate predictions than those generated at the global scale, as they can integrate higher-quality environmental data that may be available at finer spatial scales.

Sampling bias can introduce spatial autocorrelation into species distribution models (de Oliveira et al., 2014). Autocorrelation between training observations and testing observations violates the classical assumption of identically and independently

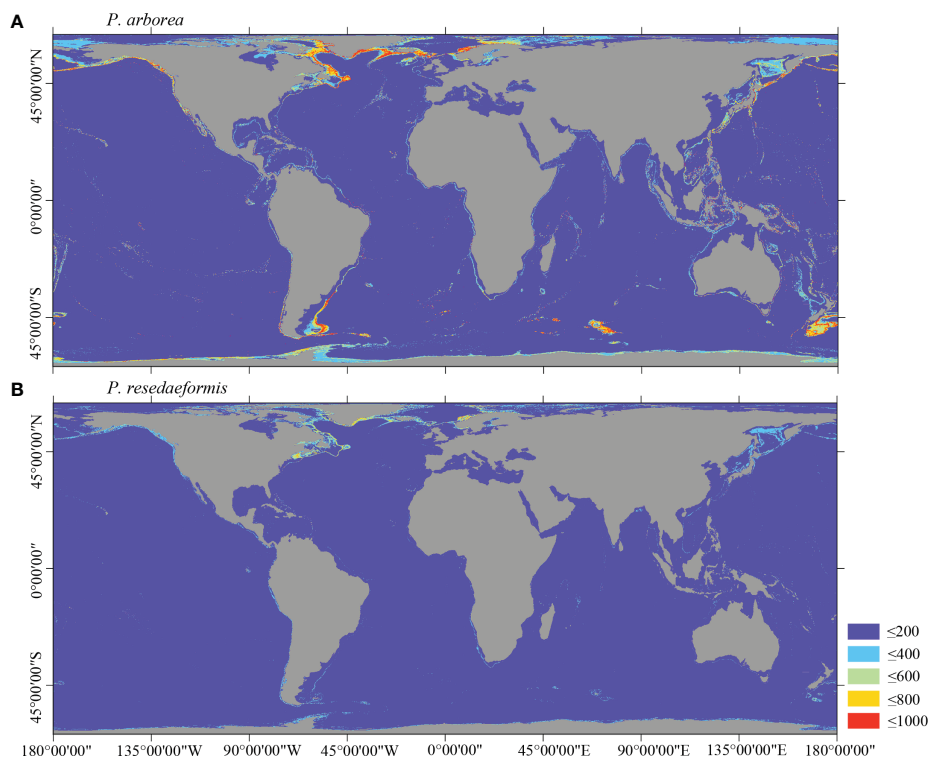


FIGURE 7

Predicted habitat suitability (0–1,000) at the global scale for cold-water corals (A) *P. arborea* and (B) *P. resedaeformis* using ensemble modeling. Warmer colors show areas of high habitat suitability.

distributed data commonly used in machine learning (Beigaite et al., 2022), which may induce autocorrelated model residuals, introducing biases in model parameter estimates and over-optimistic assessment of model predictive power, particularly in the case of highly clustered sampling (Ploton et al., 2020). In this study, sampling bias is evident, as cold-water coral presence records are abundant in the North Atlantic and South Pacific, but scarce in the North Pacific and Indian Ocean. Various spatial cross-validation strategies have been developed aiming to create independence between cross-validation folds (Roberts et al., 2017; Beigaite et al., 2022; Valavi et al., 2023). However, Wadoux et al. (2021) argue that spatial cross-validation leads to under-representation of environmental conditions similar to those at validation locations, and is likely to be over-pessimistic if there are significant differences in environmental conditions between validation and calibration folds (Wadoux et al., 2021). In this study, the predictive performance for most of the species (8 out of 10) was relatively stable, with all AUC > 0.8 and an SD  $\leq 0.057$ . However, one run in the RF prediction for *G. dumosa* yielded an AUC of 0.748, while the others were >0.8. This pattern was also observed in the models for *A. arbuscula*, with the most variable and lowest mean Continuous Boyce Indexes of 0.616 for GBM prediction and 0.693 for RF prediction, indicating positive correlation between the models' predictions and the observed presences on average. Overall, the models demonstrated good performance. However, the evaluation results of *G. dumosa* and *A. arbuscula* predictions indicate an over-pessimistic trend in the

predictive runs with low AUC values. This is likely attributed to significant differences in environmental conditions between corresponding validation and calibration folds. Increasing the number of folds can play a role in reducing the disparity between folds, thereby enhancing SDM and validation. It is important to improve cross-validation strategies by creating independent validation and calibration folds and minimize the differences between them to help avoid over-optimistic and over-pessimistic evaluations in SDM.

## 4.2 Important variables in predictions and environmental niches

As in many regional and global-scale distribution studies of cold-water corals, depth and temperature were identified as the most important environmental variables in predictions (Davies and Guinotte, 2011; Barbosa et al., 2020; Burgos et al., 2020; Tong et al., 2022). Depth was most often found to strongly influence cold-water coral distribution (Auscavitch et al., 2020), as well as other benthic fauna (Friedlander et al., 2021; Saeedi et al., 2022). Temperature was also found to be an important variable as it has a significant effect on metabolic functions through an influence in respiration and excretion rates, constraining distributions (Gomez et al., 2022). The importance of salinity also remains consistent with previous studies (Davies and Guinotte, 2011; Yesson et al., 2012), particularly for Scleractinians (*G. dumosa*, *D. pertusum*, *E. rostrata* and *O.*

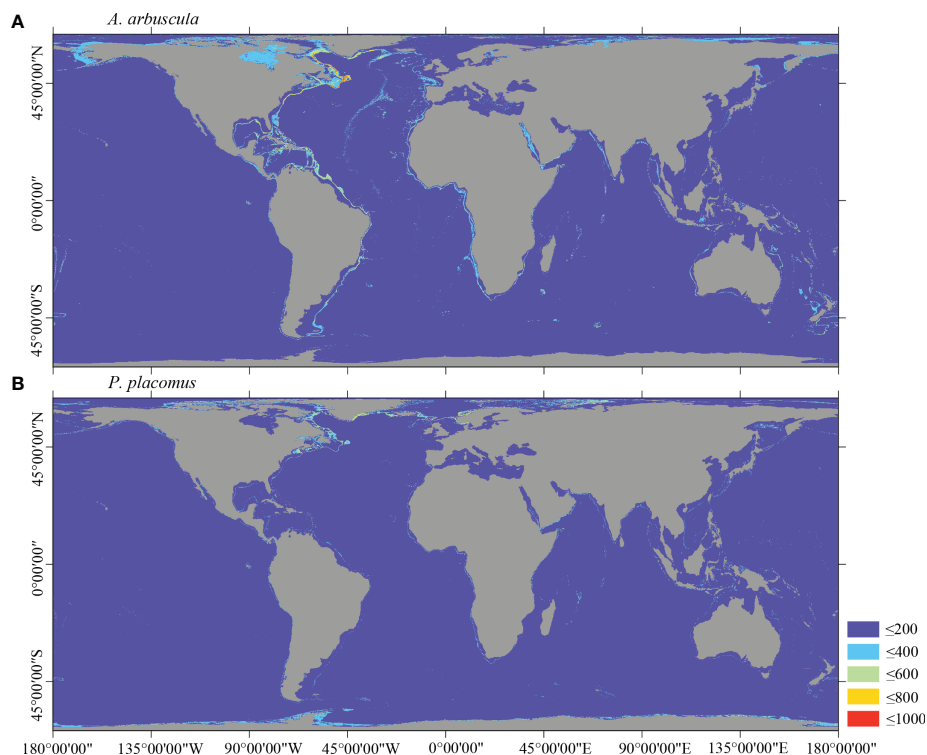


**FIGURE 8**  
 Predicted habitat suitability (0–1,000) at the global scale for cold-water corals (A) *A. arbuscula* and (B) *P. placomus* using ensemble modeling. Warmer colors show areas of high habitat suitability.

*varicosa*). Omega calcite was among the top three important variables for two out of four Octocorallia species, again consistent with previous studies (Yesson et al., 2012; Barbosa et al., 2020). Although omega aragonite showed less importance than many other variables for Scleractinians, these species predominantly inhabit saturated and supersaturated waters, reflecting the importance of saturation state for the formation of Scleractinian skeletons (Figure 3E) (Guinotte et al., 2006b; Medina et al., 2006).

Terrain variables such as TRI and slope were among the top contributors for many species, likely due to the enhanced bathymetric resolution of the global-scale model. Seabed topography is known to significantly influence the distributions of cold-water corals by altering current velocity, food particle supply, and sedimentation rates (Mortensen and Buhl-Mortensen, 2005; Davies et al., 2009). Many studies have highlighted relationships between coral presence and terrain variables such as bathymetric position index and slope, primarily at the local scale (resolution of tens of meters) (Rowden et al., 2017; Bargain et al., 2018) and regional scale (Burgos et al., 2020; Matos et al., 2021). However, these relationships have been rarely found in global-scale models for cold-water corals (Davies et al., 2008; Davies and Guinotte, 2011; Yesson et al., 2012; Yesson et al., 2017). Our findings suggest that with increased data resolution, particularly with respect to bathymetry, these finer-scale distributional controls can be captured in broad-scale

distribution models and play an important role in driving the distribution patterns of cold-water corals across oceans.

Cold-water corals are sessile filter feeders that rely on organic matter and zooplankton brought to them by currents or food particles transported from the surface (Soetaert et al., 2016; van Oevelen et al., 2016). This food supply is largely controlled by export production at the surface, lateral advection, and turbulent hydrodynamics. In a recent study, such processes were found to have exerted the strongest impact on coral vitality across the past 20,000 years in North Atlantic and the Mediterranean Sea (Portilho-Ramos et al., 2022). In our models, chlorophyll concentration was important for 3 out of 10 species, particularly for the Octocorals, *P. arborea*, and *P. resedaeformis* (Table 3). Additionally, these species exhibited a tendency towards areas with higher mean chlorophyll, indicating potentially elevated food supply requirements (Figure 4C). Current velocity, especially when modeled at high resolution, has also been found to considerably improve the performance of predictive models and play a crucial role in predicting local-scale cold-water coral distribution (Rengstorf et al., 2012; Bargain et al., 2018; Dolan et al., 2021). However, previous global-scale studies did not detect such a relationship (Davies et al., 2008; Tittensor et al., 2009; Yesson et al., 2012). In this study, current velocity emerged as important for two species, which again is likely linked to the inclusion of a higher-resolution layer that better reflects local current variation.

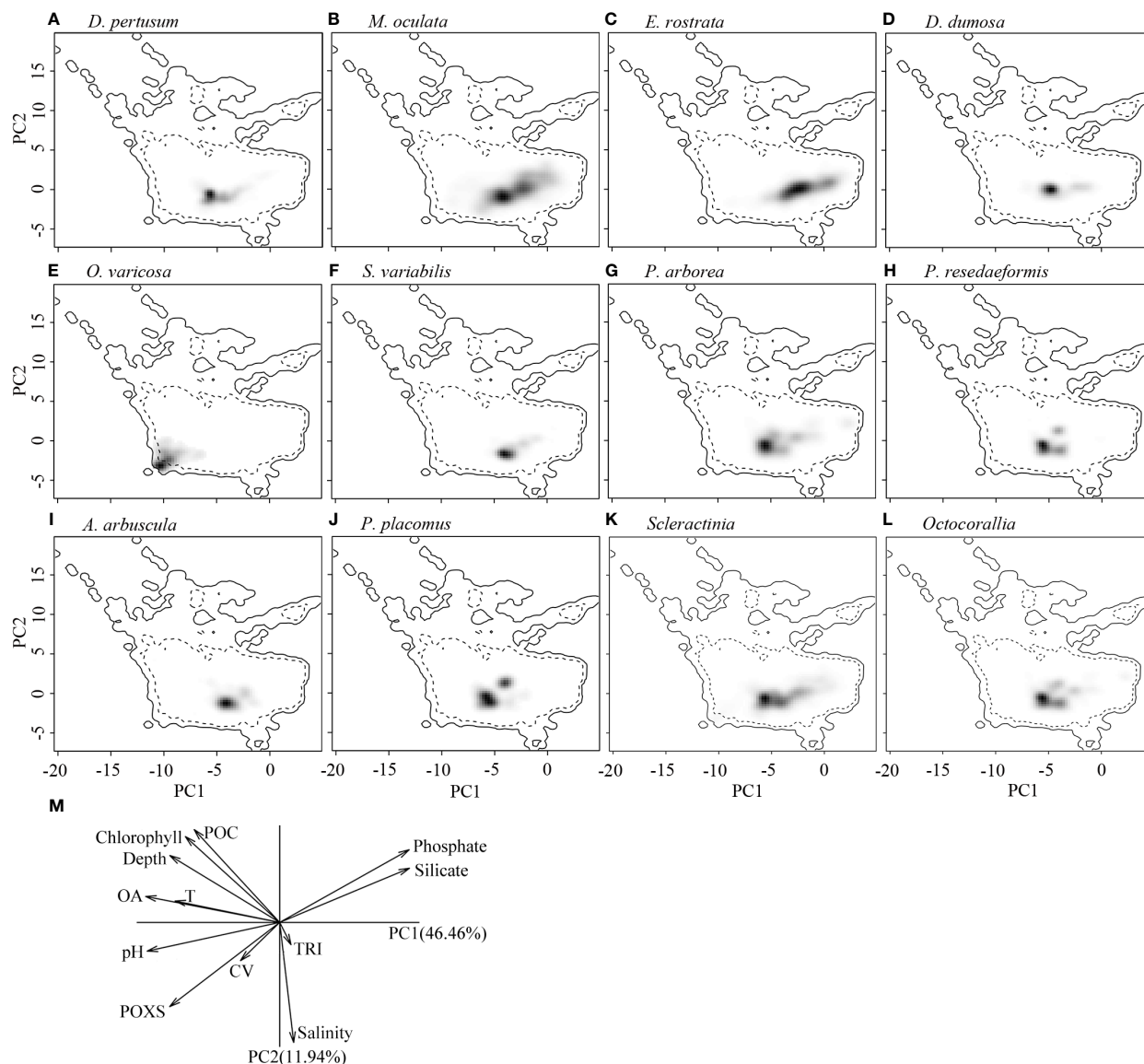


FIGURE 9

Estimated ecological niches of the 10 cold-water coral species, Scleractinia, and Octocorallia by principal component analysis, with the environmental space determined by the axes of PC1 and PC2 (A–L). The gray to black shading represents the kernel density of species presence, with black showing the highest density. The solid lines represent the 100% of available environmental conditions within the global ocean environmental data, while dashed lines represent 50% of available environmental conditions. (M) shows the contribution of each variable to the two principal components in ecological niche analysis using principal component analysis, with omega aragonite used to express water carbonate conditions. POXS, percentage oxygen saturation; OA, omega aragonite; POC, particulate organic carbon; T, temperature; TRI, terrain ruggedness index; CV, current velocity.

### 4.3 Predicted habitat suitability

This study extends global predictions for cold-water corals into areas omitted from previous studies such as latitudes greater than 60°N, the Gulf of Mexico, the South China Sea, and the Mediterranean Sea (Davies et al., 2008; Davies and Guinotte, 2011). The North Atlantic beyond 60°N was found to contain suitable habitat for *D. pertusum*, *P. arborea*, *P. resedaeformis*, and *P. placomus*, as was the Mediterranean Sea and Red Sea for *M. oculata*, *D. pertusum*, and *E. rostrata*, and Gulf of Mexico and the Caribbean Sea for *S. variabilis*, *M. oculata*, *E. rostrata*, *D. pertusum*, and *A. arbuscula*, consistent with previous studies (Yesson et al., 2012;

Burgos et al., 2020; Morato et al., 2020; Matos et al., 2021). In addition, high habitat suitability for *D. pertusum* and *M. oculata* was predicted in the Cabliers Coral Mounds areas in the West Mediterranean Sea in this study, which agrees with current knowledge that Cabliers is the only known coral mound province in the Mediterranean Sea with currently growing reefs (Corbera et al., 2019). The South China Sea to North Australia region was predicted to contain expanses of suitable habitat for *M. oculata*, *E. rostrata*, *G. dumosa*, and *S. variabilis*. These findings are also supported by a previous study that revealed that the region bordered to the north of the Philippines and to the SE by New Caledonia, including New Guinea and the NE coast of Australia,

TABLE 5 Niche comparison for each pair of the 10 species using Schoener's D, with the upper triangle representing niche overlap (D) and the lower triangle representing the *p*-value of niche similarity.

	<i>D. pertusum</i>	<i>M. oculata</i>	<i>E. rostrata</i>	<i>G. dumosa</i>	<i>O. varicosa</i>	<i>S. variabilis</i>	<i>P. arborea</i>	<i>P. resedaeformis</i>	<i>A. arbuscula</i>	<i>P. placomus</i>
<i>D. pertusum</i>		0.43	0.29	0.32	0.01	0.19	0.64	0.70	0.25	0.67
<i>M. oculata</i>	NS		0.51	0.31	0.02	0.26	0.47	0.34	0.34	0.29
<i>E. rostrata</i>	NS	NS		0.29	0.00	0.31	0.35	0.27	0.39	0.21
<i>G. dumosa</i>	NS	NS	NS		0.00	0.15	0.43	0.33	0.30	0.30
<i>O. varicosa</i>	NS	NS	NS	NS		0.00	0.00	0.00	0.00	0.00
<i>S. variabilis</i>	NS	NS	NS	NS	NS		0.20	0.22	0.64	0.11
<i>P. arborea</i>	NS	NS	NS	NS	NS	NS		0.66	0.33	0.61
<i>P. resedaeformis</i>	0.0396	NS	NS	NS	NS	NS	NS		0.32	0.75
<i>A. arbuscula</i>	NS	NS	NS	NS	NS	NS	NS	NS		0.20
<i>P. placomus</i>	0.0495	NS	NS	NS	NS	NS	NS	0.0099	NS	

Schoener's D ranges from 0 (none overlap) to 1 (complete overlap). *p*-values of niche similarity or niche equivalency  $\leq 0.05$  indicate falling outside the 95% confidence interval of the niche similarity test or niche equivalency test. The *p*-value of niche similarity  $\leq 0.05$  was shown as number, and shown as NS (no significant similarity) otherwise. The niche overlap between Scleractinia and Octocorallia cold-water corals is 0.30, also with no significant similarity. The *p*-value of niche equivalency of each pair tested is equal to 1, and not shown in the table. The gray section serves no significant purpose; it is simply for improved readability.

may be the most diverse center of the global ocean for Scleractinian cold-water corals, with the Caribbean Sea and Gulf of Mexico also being highly diverse (Cairns, 2007). Our models also indicated a high level of habitat suitability on certain regions of continental shelf margins for all species (Cordeiro et al., 2020), again consistent with previous studies (Davies and Guinotte, 2011; Yesson et al., 2012).

*Oculina varicosa* had the smallest area of predicted habitat suitability. Suitable habitat for *M. oculata* was most widely distributed throughout the global ocean, followed by *E. rostrata*, which showed an increase in potential distribution over previous studies (Davies and Guinotte, 2011). These widespread distributions indicate that the species may be found in a broad range of physical-chemical environment conditions (Slatyer et al., 2013). *Solenosmilia variabilis* was predicted to be globally distributed, with high habitat suitability in the North Atlantic and around the Caribbean Sea and Gulf of Mexico, particularly along the Mid-Ocean Ridge, and in the South Pacific. The result is in line with several regional studies, which predicted the high habitat suitability on large ridges and around the Campbell Plateau (Anderson et al., 2016; Georgian et al., 2019; Stephenson et al., 2021b; Anderson et al., 2022), and also on the New Zealand margin (Georgian et al., 2019), as well as on the Louisville Seamount Chain in New Zealand waters (Rowden et al., 2017). However, in a previous study, the waters surrounding New Zealand was predicted as the most suitable habitat (Davies and Guinotte, 2011), in contrast to the present study that observed less suitable habitat in this region. Such an increase in potential habitat suitability outside of New Zealand is likely due to the increase in the number and geographic extent of observation records used in this study, resulting in a better representation of the environmental niche by incorporating a broader range of environmental conditions than previously recorded.

In this study, a greater number of seamounts and areas surrounding oceanic islands were predicted to contain suitable

habitat for cold-water corals (Supplementary Figures 3–6), representing an increase in detectability over previous global studies where only larger seamounts were identified (Davies et al., 2008; Tittensor et al., 2009; Davies and Guinotte, 2011; Yesson et al., 2012; Yesson et al., 2017). This was particularly evident for the Scleractinian species *M. oculata*, *E. rostrata*, *D. pertusum*, and *S. variabilis*, as well as the gorgonian *P. arborea*. Deep-sea canyons, seamounts, and ridges are well known as biological hotspots, including for cold-water corals, as they provide hard substrate and accelerate current velocities that act to enhance food supply and reduce sedimentation loading on reefs (Robert et al., 2019; Auscavitch et al., 2020; Georgian et al., 2021). In addition, these topographically complex features can interact with tidal currents causing downwelling events of organic matter from surface water, forming a “topographically enhanced carbon pump”, to increase food supply to depth, which is essential for the persistence of cold-water corals in the deep sea (Davies et al., 2009; Soetaert et al., 2016; van Oevelen et al., 2016).

The predicted suitable habitat largely reflects a similar distribution pattern to presence locations for each species (Supplementary Figures 3–6, Figure 1). All of the predicted suitable habitat areas are limited to depths shallower than the maximum depth of the corresponding species' presence. However, there are predicted suitable habitat areas where there are no currently known observations, for example, areas off the SW Africa for *G. dumosa*, and off the NE South America for *O. varicosa*. These areas often exhibit a relatively higher level of uncertainty (Supplementary Figures 4, 7). Caution should be employed in considering those areas as suitable habitat for those species, and further field sampling is needed to validate predicted habitat suitability in these regions. Only few areas of the predicted suitable habitat were covered by MPAs throughout the global ocean (Supplementary Figure 8) (IUCN U-Wa, 2023). Therefore, large areas, mainly on the continental shelf should be further

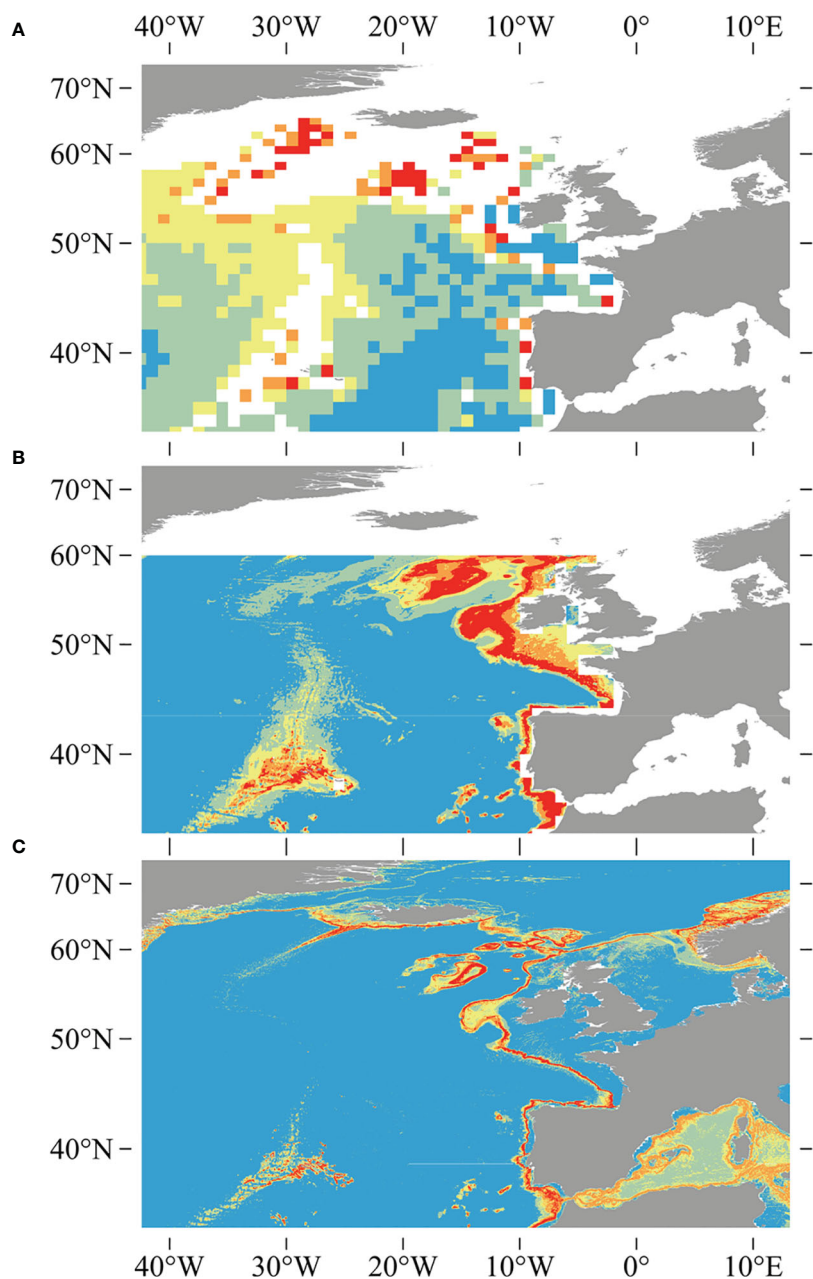


FIGURE 10

Comparisons between earlier studies of outputs for *D. pertusum*, including (A) the global model created using ecological niche factor analysis in Davies et al. (2008), (B) the model created using the Maxent modeling approach and 1,000-m-resolution bathymetry in Davies and Guinotte (2011), and (C) the model generated using 500-m-resolution bathymetry and an ensemble modeling approach in this study. Note reduction in over-prediction and increase in resolution of this study relative to earlier studies.

investigated and considered as priority regions for the conservation and management of these vulnerable species.

#### 4.4 Ecological niche analysis

None of the 10 species investigated in this study shared an equivalent niche, as evidenced by the wide variation in environmental conditions where these 10 species occur. However,

*S. variabilis* and *A. arbuscula* were found to share a high level niche overlap (0.64) in this study. Both *S. variabilis* and *A. arbuscula* are often observed in the North Atlantic and in waters surrounding New Zealand. However, *S. variabilis* is a typical reef-forming Scleractinian found on both mixed and hard seabed (Mortensen et al., 2008), while *A. arbuscula* is a soft sediment specialist that is seen on muddy and mixed seabed (Edinger et al., 2011). Although these species overlap in their preference for mixed substrates, this niche high level niche overlap is likely linked to some sampling bias

away from areas where just one species is present, such as vertical walls for *S. variabilis* (Davies et al., 2017) and deeper mud flats for *A. arbuscula* (Long et al., 2021). Substrate is an important factor determining coral distributions, but no global substrate maps are available for the seabed, and this remains an ongoing limitation for SDMs of benthic organisms constructed at regional scales and larger.

There is a high level degree of overlap between the niches of *D. pertusum*, *P. arborea*, *P. resedaeformis*, and *P. placomus*, indicating potential shared adaptations to certain environmental conditions. The highest overlap was observed between *P. resedaeformis* and *P. placomus*, *D. pertusum* and *P. lacomus*, *D. pertusum* and *P. resedaeformis*, which pairs share similar niches. *Paragorgia arborea*, *P. resedaeformis*, and *P. placomus* are often observed within *D. pertusum* reefs, particularly on the Norwegian margin (Buhl-Mortensen et al., 2015), underscoring the necessity of protecting cold-water coral reefs as a habitat. The species with the most distinct niche was *O. varicosa*, which demonstrated the least overlap with other species. The result is in line with known knowledge that *O. varicosa* is predominantly found in shallower waters and has zooxanthellae symbionts at depths shallower than -60 m (Reed, 2002), whereas all other species lack algal symbionts. This highlights the need for implementing targeted measures for the conservation of specific species.

As reflected in the geographic extent of potential suitable habitat for *M. oculata*, the niche breadth of *M. oculata* was significantly larger than that of other species. This may indicate that *M. oculata* is possibly less sensitive to climatic change, whereas the narrower niches of other species, such as *P. resedaeformis*, may make them more susceptible to such change (Barbosa et al., 2020). Furthermore, the high-latitude distribution of *P. resedaeformis* and other northern species with relatively narrow niches places these potentially less resilient species in an area of rapid environmental change (Overland et al., 2019), further highlighting the need for targeted conservation efforts in these areas.

## 5 Conclusion

Our results provide valuable and updated information for the global habitat suitability for six cold-water reef-framework forming Scleractinian species and four large cold-water gorgonian species. Our models and analyses can contribute to ongoing efforts to map vulnerable marine ecosystems, enable more informed decisions in the development of marine protected areas, and support UN Sustainable Development Goal 14: Conserve and sustainably use the oceans, seas and marine resources (United Nations, 2015), which aims to protect the aquatic organism from the challenges such as ocean warming, ocean acidification, and anthropogenic impacts by 2030. Our models provide a much-needed update on earlier global distribution modeling efforts for cold-water corals, which integrate the highest-resolution bathymetric grid available, along with updated environmental variables for the global ocean,

addition of new modeling approaches, and more species observations. This study ultimately represents significant improvement that has benefited from a decade of interest into mapping and characterizing the ocean and communities within.

## Data availability statement

The computer code used for constructing the 11 environmental variables in this study are available on GitHub (<https://github.com/marecotec/GlobENV>). The 11 environmental layers created in this study are publicly accessible through the Zenodo data publisher portal (<https://zenodo.org/record/8336590>). Additionally, the predicted habitat suitability maps can be downloaded from Zenodo (<https://zenodo.org/record/7896310>).

## Ethics statement

The manuscript presents research on animals that do not require ethical approval for their study.

## Author contributions

RT, AD, and CY contributed to the conception and design of the study. RT, JY, YL, and LZ preprocessed the data, created the codes, performed the modeling, and provided the statistical analysis. AD calculated the updated environmental variables and spatial validation. The manuscript was written by RT, and was contributed to and edited by AD, CY, and JMB. All authors contributed to the revision of the manuscript and approved the final submission.

## Funding

This research was supported by the National Natural Science Foundation of China (No. 42006140), the National Key R&D Program of China (No. 2019YFE0127100), and the Natural Science Foundation of Fujian Province of China (No. 2019I0006). AD was partly funded by the USDA National Institute of Food and Agriculture, Hatch Formula project accession number 1017848. Staff at ZSL Institute of Zoology is supported by funding from Research England. JMB is funded by the Ministry of Food, Agriculture and Fisheries, Government of Iceland.

## Acknowledgments

We thank Dr. Chih-Lin Wei from National Taiwan University for providing particulate organic carbon data and two reviewers for their valuable feedback.

## Conflict of interest

The authors declare that the research was conducted in the absence of any commercial or financial relationships that could be construed as a potential conflict of interest.

## Publisher's note

All claims expressed in this article are solely those of the authors and do not necessarily represent those of their affiliated

organizations, or those of the publisher, the editors and the reviewers. Any product that may be evaluated in this article, or claim that may be made by its manufacturer, is not guaranteed or endorsed by the publisher.

## Supplementary material

The Supplementary Material for this article can be found online at: <https://www.frontiersin.org/articles/10.3389/fmars.2023.1217851/full#supplementary-material>

## References

- Addamo, A. M., Vertino, A., Stolarski, J., Garcia-Jimenez, R., Taviani, M., and Machordom, A. (2016). Merging Scleractinian genera: the overwhelming genetic similarity between solitary *Desmophyllum* and colonial *Lophelia*. *BMC Evolutionary Biol.* 16. doi: 10.1186/s12862-016-0654-8
- Aguirre-Gutiérrez, J., Serna-Chavez, H. M., Villalobos-Arambula, A. R., Pérez de la Rosa, J. A., and Raes, N. (2015). Similar but not equivalent: ecological niche comparison across closely-related Mexican white pines. *Diversity Distributions* 21, 245–257. doi: 10.1111/ddi.12268
- Anderson, O. F., Guinotte, J. M., Rowden, A. A., Tracey, D. M., Mackay, K. A., and Clark, M. R. (2016). Habitat suitability models for predicting the occurrence of vulnerable marine ecosystems in the seas around New Zealand. *Deep Sea Res. Part I: Oceanographic Res. Papers* 115, 265–292. doi: 10.1016/j.dsr.2016.07.006
- Anderson, O. F., Stephenson, F., Behrens, E., and Rowden, A. A. (2022). Predicting the effects of climate change on deep-water coral distribution around New Zealand—Will there be suitable refuges for protection at the end of the 21st century? *Global Change Biol.* 28, 6556–6576. doi: 10.1111/gcb.16389
- Araújo, M. B., Anderson, R. P., Barbosa, A. M., Beale, C. M., Dormann, C. F., Early, R., et al. (2019). Standards for distribution models in biodiversity assessments. *Sci. Adv.* 5. doi: 10.1126/sciadv.aat4858
- Assis, J., Tyberghein, L., Bosch, S., Verbruggen, H., Serrão, E. A., and De Clerck, O. (2018). Bio-ORACLE v2.0: Extending marine data layers for bioclimatic modelling. *Global Ecol. Biogeography* 27, 277–284. doi: 10.1111/geb.12693
- Auscavitch, S. R., Lunden, J. J., Barkman, A., Quattrini, A. M., Demopoulos, A. W. J., and Cordes, E. E. (2020). Distribution of deep-water Scleractinian and Styliasterid corals across abiotic environmental gradients on three seamounts in the Anegada Passage. *PeerJ* 8. doi: 10.7717/peerj.9523
- Barbosa, R. V., Davies, A. J., and Sumida, P. Y. G. (2020). Habitat suitability and environmental niche comparison of cold-water coral species along the Brazilian continental margin. *Deep-Sea Res. Part I: Oceanographic Res. Papers* 155. doi: 10.1016/j.dsr.2019.103147
- Bargain, A., Fogliani, F., Pairaud, I., Bonaldo, D., Carniel, S., Angeletti, L., et al. (2018). Predictive habitat modeling in two Mediterranean canyons including hydrodynamic variables. *Prog. Oceanography* 169, 151–168. doi: 10.1016/j.pocean.2018.02.015
- Beigaitte, R., Mechenich, M., and Zliobaite, I. (2022). “Spatial Cross-Validation for Globally Distributed Data 25th International Conference on Discovery Science (DS),” 25th International Conference on Discovery Science 2022 (Cham, Montpellier: Springer), 127–140.
- Boria, R. A., Olson, L. E., Goodman, S. M., and Anderson, R. P. (2014). Spatial filtering to reduce sampling bias can improve the performance of ecological niche models. *Ecol. Model.* 275, 73–77. doi: 10.1016/j.ecolmodel.2013.12.012
- Boyer, T., Levitus, S., Garcia, H., Locarnini, R. A., Stephens, C., and Antonov, J. (2005). Objective analyses of annual, seasonal, and monthly temperature and salinity for the World Ocean on a 0.25° grid. *Int. J. Climatology* 25, 931–945. doi: 10.1002/joc.1173
- Breiman, L. (2001). Random forests. *Mach. Learn.* 45, 5–32. doi: 10.1023/A:1010933404324
- Broenniman, O., Di Cola, V., and Guisan, A. (2022). *ecospat: Spatial Ecology Miscellaneous Methods. R package version 34*. Available at: <https://CRAN.R-project.org/package=ecospat>.
- Broennimann, O., Fitzpatrick, M. C., Pearman, P. B., Petitpierre, B., Pellissier, L., Yoccoz, N. G., et al. (2012). Measuring ecological niche overlap from occurrence and spatial environmental data. *Global Ecol. Biogeography* 21, 481–497. doi: 10.1111/j.1466-8238.2011.00698.x
- Buhl-Mortensen, L., Mortensen, P. B., Freiwald, A., and Roberts, J. M. (2005). “Distribution and diversity of species associated with deep-sea gorgonian corals off Atlantic Canada,” in *Cold-water corals and ecosystems*. Eds. A. Freiwald and J. M. Roberts (Berlin Heidelberg: Springer), 849–879.
- Buhl-Mortensen, L., Olafsdottir, S. H., Buhl-Mortensen, P., Burgos, J. M., and Ragnarsson, S. A. (2015). Distribution of nine cold-water coral species (Scleractinia and Gorgonacea) in the cold temperate North Atlantic: effects of bathymetry and hydrography. *Hydrobiologia* 759, 39–61. doi: 10.1007/s10750-014-2116-x
- Buhl-Mortensen, L., Vanreusel, A., Gooday, A., Levin, L., Priede, I., Buhl-Mortensen, P., et al. (2010). Biological structures as a source of habitat heterogeneity and biodiversity on the deep ocean margins. *Mar. Ecol.* 31, 21–50. doi: 10.1111/j.1439-0485.2010.00359.x
- Burgos, J. M., Buhl-Mortensen, L., Buhl-Mortensen, P., Olafsdottir, S. H., Steingrund, P., Ragnarsson, S. A., et al. (2020). Predicting the distribution of indicator taxa of vulnerable marine ecosystems in the arctic and sub-arctic waters of the nordic seas. *Front. Mar. Sci.* 7. doi: 10.3389/fmars.2020.00131
- Cairns, S. D. (2007). Deep-sea corals: an overview with special reference to diversity and distribution of deep-water Scleractinian corals. *Bull. Mar. Sci.* 81, 311–322.
- Connor, T., Hull, V., Vina, A., Shortridge, A., Tang, Y., Zhang, J. D., et al. (2018). Effects of grain size and niche breadth on species distribution modeling. *Ecography* 41, 1270–1282. doi: 10.1111/ecog.03416
- Corbera, G., Iacono, C. L., Gracia, E., Grinyo, J., Pierdomenico, M., Huvenne, V., et al. (2019). Ecological characterisation of a Mediterranean cold-water coral reef: Cabliers Coral Mound Province (Alboran Sea, western Mediterranean). *Prog. In Oceanography* 175, 245–262. doi: 10.1016/j.pocean.2019.04.010
- Cordeiro, R. T. S., Neves, B. M., Kitahara, M. V., Arantes, R. C. M., and Perez, C. D. (2020). First assessment on Southwestern Atlantic equatorial deep-sea coral communities. *Deep-Sea Res. Part I: Oceanographic Res. Papers* 163. doi: 10.1016/j.dsr.2020.103344
- Davies, A. J., Duineveld, G. C. A., Lavaleye, M. S. S., Bergman, M. J. N., van Haren, H., and Roberts, J. M. (2009). Downwelling and deep-water bottom currents as food supply mechanisms to the cold-water coral *Lophelia pertusa* (Scleractinia) at the Mingulay Reef Complex. *Limnology Oceanography* 54, 620–629. doi: 10.4319/lo.2009.54.2.0620
- Davies, A. J., and Guinotte, J. M. (2011). Global habitat suitability for framework-forming cold-water corals. *PLoS One* 6. doi: 10.1371/journal.pone.0018483
- Davies, A., Wisshak, M., Orr, J., and Roberts, J. (2008). Predicting suitable habitat for the cold-water coral *Lophelia pertusa* (Scleractinia). *Deep-Sea Res. Part I: Oceanographic Res. Papers* 55, 1048–1062. doi: 10.1016/j.dsr.2008.04.010
- Davies, J. S., Guillaumont, B., Tempera, F., Vertino, A., Beuck, L., Olafsdottir, S. H., et al. (2017). A new classification scheme of European cold-water coral habitats: Implications for ecosystem-based management of the deep sea. *Deep-Sea Res. Part II: Topical Stud. Oceanography* 145, 102–109. doi: 10.1016/j.dsr2.2017.04.014
- de Froe, E., Rovelli, L., Glud, R. N., Maier, S. R., Duineveld, G., Mienis, F., et al. (2019). Benthic oxygen and nitrogen exchange on a cold-water coral reef in the north-east Atlantic ocean. *Front. Mar. Sci.* 6. doi: 10.3389/fmars.2019.00665
- de Oliveira, G., Rangel, T. F., Lima-Ribeiro, M. S., Terribile, L. C., and Felizola Diniz-Filho, J. A. (2014). Evaluating, partitioning, and mapping the spatial autocorrelation component in ecological niche modeling: a new approach based on environmentally equidistant records. *Ecography* 37, 637–647. doi: 10.1111/j.1600-0587.2013.00564.x
- Di Cola, V., Broennimann, O., Petitpierre, B., Breiner, F. T., D’Amen, M., Randin, C., et al. (2017). *ecospat: an R package to support spatial analyses and modeling of species niches and distributions*. *Ecography* 40, 774–787. doi: 10.1111/ecog.02671
- Dolan, M., Ross, R., Albreten, J., Skardhamar, J., Gonzalez-Mirelis, G., Bellec, V., et al. (2021). Using spatial validity and uncertainty metrics to determine the relative suitability of alternative suites of oceanographic data for seabed biotope prediction. A

- case study from the barents sea, Norway. *Geosciences* 11. doi: 10.3390/geosciences11020048
- Edinger, E. N., Sherwood, O. A., Piper, D. J. W., Wareham, V. E., Baker, K. D., Gilkinson, K. D., et al. (2011). Geological features supporting deep-sea coral habitat in Atlantic Canada. *Continental Shelf Res.* 31, 69–84. doi: 10.1016/j.csr.2010.07.004
- Elith, J., Graham, C. H., Anderson, R. P., Dudik, M., Ferrier, S., Guisan, A., et al. (2006). Novel methods improve prediction of species' distributions from occurrence data. *Ecography* 29, 129–151. doi: 10.1111/j.2006.0906-7590.04596.x
- Elith, J., Kearney, M., and Phillips, S. (2010). The art of modelling range-shifting species. *Methods Ecol. Evol.* 1, 330–342. doi: 10.1111/j.2041-210X.2010.00036.x
- Fitzpatrick, M. C., Gotelli, N. J., and Ellison, A. M. (2013). MaxEnt versus MaxLike: empirical comparisons with ant species distributions. *Ecosphere* 4, 1–15. doi: 10.1890/ES13-00066.1
- Freiwald, A., Fosså, J. H., Grehan, A., Koslow, T., and Roberts, J. M. (2004). Cold-water coral reefs: out of sight-no longer out of mind. *UNEP-WCMC*, 86.
- Friedlander, A. M., Goodell, W., Giddens, J., Easton, E. E., and Wagner, D. (2021). Deep-sea biodiversity at the extremes of the Salas y Gomez and Nazca ridges with implications for conservation. *PLoS One* 16. doi: 10.1371/journal.pone.0253213
- Friedman, J. H. (2001). Greedy function approximation: A gradient boosting machine. *Ann. Stat.* 29, 1189–1232. doi: 10.1214/aos/1013203451
- Garcia, H. E., Locarnini, R. A., Boyer, T. P., and Antonov, J. I. (2006a). "World Ocean Atlas 2005, Volume 4: Nutrients (phosphate, nitrate, silicate)," in NOAA atlas NESDIS 64, U.S. Ed. S. Levitus (Washington DC: Government Printing Office), 396 p.
- Garcia, H. E., Locarnini, R. A., Boyer, T. P., and Antonov, J. I. (2006b). "World ocean atlas 2005, volume 3: dissolved oxygen, apparent oxygen utilization, and oxygen saturation," in NOAA atlas NESDIS 63, U.S. Ed. S. Levitus (Washington DC: Government Printing Office), 342.
- Garcia, H. E., Weathers, K. W., Paver, C. R., Smolyar, I., Boyer, T. P., Locarnini, R. A., et al. (2018a). *World ocean atlas 2018, volume 3: dissolve oxygen, apparent oxygen utilization, and dissolved oxygen saturation* (A. Mishonov Technical Editor), 26. NOAA Atlas NESDIS 83, Silver Spring.
- Garcia, H. E., Weathers, K. W., Paver, C. R., Smolyar, I., Boyer, T. P., Locarnini, R. A., et al. (2018b). *World Ocean Atlas 2018. Volume 4: Dissolved Inorganic Nutrients (phosphate, nitrate and nitrate+nitrite, silicate)* (Mishonov, A. Technical Editor), 24. NOAA Atlas NESDIS 84, Silver Spring.
- Gattuso, J.-P., Epitalon, J.-M., Lavigne, H., and Orr, J. (2022). *seacarb: seawater carbonate chemistry. R package version 3.3.1*. Available at: <http://CRAN.R-project.org/package=seacarb>.
- GEBCO Compilation Group (2022). *GEBCO\_2022*. doi: 10.5285/e0f0bb80-ab44-2739-e053-6c86abc0289c
- Georgian, S. E., Anderson, O. F., and Rowden, A. A. (2019). Ensemble habitat suitability modeling of vulnerable marine ecosystem indicator taxa to inform deep-sea fisheries management in the South Pacific Ocean. *Fisheries Res.* 211, 256–274. doi: 10.1016/j.fishres.2018.11.020
- Georgian, S. E., Kramer, K., Saunders, M., Shedd, W., Roberts, H., Lewis, C., et al. (2020). Habitat suitability modelling to predict the spatial distribution of cold-water coral communities affected by the Deepwater Horizon oil spill. *J. Biogeography* 47, 1455–1466. doi: 10.1111/jbi.13844
- Georgian, S., Morgan, L., and Wagner, D. (2021). The modeled distribution of corals and sponges surrounding the Salas y Gomez and Nazca ridges with implications for high seas conservation. *PeerJ* 9. doi: 10.7717/peerj.11972
- Gomez, C. E., Gori, A., Weinnig, A. M., Hallaj, A., Chung, H. J., and Cordes, E. E. (2022). Natural variability in seawater temperature compromises the metabolic performance of a reef-forming cold-water coral with implications for vulnerability to ongoing global change. *Coral Reefs* 41, 1225–1237. doi: 10.1007/s00338-022-02267-2
- Grimmett, L., Whitted, R., and Horta, A. (2020). Presence-only species distribution models are sensitive to sample prevalence: Evaluating models using spatial prediction stability and accuracy metrics. *Ecol. Model.* 431. doi: 10.1016/j.ecolmodel.2020.109194
- Guinotte, J. M., Bartley, J. D., Iqbal, A., Fautin, D. G., and Buddemeier, R. W. (2006b). Modeling habitat distribution from organism occurrences and environmental data: case study using anemonefishes and their sea anemone hosts. *Mar. Ecol. Prog. Ser.* 316, 269–283. doi: 10.3354/meps316269
- Guinotte, J. M., and Davies, A. J. (2014). Predicted deep-sea coral habitat suitability for the US west coast. *PLoS One* 9. doi: 10.1371/journal.pone.0093918
- Guinotte, J., Orr, J., Cairns, S., Freiwald, A., Morgan, L., and George, R. (2006a). Will human-induced changes in seawater chemistry alter the distribution of deep-sea Scleractinian corals? *Front. Ecol. Environ.* 4, 141–146. doi: 10.1890/1540-9295(2006)004[0141:WHCISC]2.0.CO;2
- Hall-Spencer, J., Allain, V., and Fosså, J. H. (2002). Trawling damage to Northeast Atlantic ancient coral reefs. *Proc. R. Soc. B-Biological Sci.* 269, 507–511. doi: 10.1098/rspb.2001.1910
- Heiberger, R. M. (2022). *HH: Statistical Analysis and Data Display: Heiberger and Holland. R package version*. Available at: <https://CRAN.R-project.org/package=HH>.
- Hirzel, A. H., Le Lay, G., Helfer, V., Randin, C., and Guisan, A. (2006). Evaluating the ability of habitat suitability models to predict species presences. *Ecol. Model.* 199, 142–152. doi: 10.1016/j.ecolmodel.2006.05.017
- Huang, Z., Brooke, B., and Li, J. (2011). Performance of predictive models in marine benthic environments based on predictions of sponge distribution on the Australian continental shelf. *Ecol. Inf.* 6, 205–216. doi: 10.1016/j.ecoinf.2011.01.001
- IUCN U-Wa (2023). *Protected planet: the world database on protected areas (WDPA) and world database on other effective area-based conservation measures (WD-OECM) [Online], July 2023* (Cambridge, UK: UNEP-WCMC and IUCN). Available at: [www.protectedplanet.net](http://www.protectedplanet.net).
- Khosravifard, S., Skidmore, A. K., Toxopeus, A. G., and Niamir, A. (2020). Potential invasion range of raccoon in Iran under climate change. *Eur. J. Wildlife Res.* 66. doi: 10.1007/s10344-020-01438-2
- Kvile, K. O., Taranto, G. H., Pitcher, T. J., and Morato, T. (2014). A global assessment of seamount ecosystems knowledge using an ecosystem evaluation framework. *Biol. Conserv.* 173, 108–120. doi: 10.1016/j.biocon.2013.10.002
- Lagasse, C. R., Knudby, A., Curtis, J., Finney, J. L., and Cox, S. P. (2015). Spatial analyses reveal conservation benefits for cold-water corals and sponges from small changes in a trawl fishery footprint. *Mar. Ecol. Prog. Ser.* 528, 161–172. doi: 10.3354/meps11271
- Larsson, A. I., and Purser, A. (2011). Sedimentation on the cold-water coral *Lophelia pertusa*: Cleaning efficiency from natural sediments and drill cuttings. *Mar. Pollut. Bull.* 62, 1159–1168. doi: 10.1016/j.marpolbul.2011.03.041
- Lauvset, S. K., Key, R. M., Olsen, A., van Heuven, S., Velo, A., Lin, X., et al. (2016). A new global interior ocean mapped climatology: the 1°x1° GLODAP version 2. *Earth System Sci. Data* 8, 325–340. doi: 10.5194/essd-8-325-2016
- Lauvset, S. K., Lange, N., Tanhua, T., Bittig, H., Olsen, A., Kozyr, A., et al. (2022). GLODAPv2.2022: the latest version of the global interior ocean biogeochemical data product. *Earth System Sci. Data* 14, 5543–5572.
- Liu, C. R., Newell, G., and White, M. (2016). On the selection of thresholds for predicting species occurrence with presence-only data. *Ecol. Evol.* 6, 337–348. doi: 10.1002/ece3.1878
- Locarnini, R. A., Mishonov, A. V., Baranova, O. K., Boyer, T. P., Zweng, M. M., Garcia, H. E., et al. (2018). *World ocean atlas 2018, volume 1: temperature* (A. Mishonov, Technical Editor). NOAA Atlas NESDIS 81, Silver Spring.
- Long, S., Blicher, M. E., Arboe, N. H., Fuhrmann, M., Darling, M., Kemp, K. M., et al. (2021). Deep-sea benthic habitats and the impacts of trawling on them in the offshore Greenland halibut fishery, Davis Strait, west Greenland. *Ices J. Mar. Sci.* 78, 2724–2744. doi: 10.1093/icesjms/fsab148
- Lutz, M., Caldeira, K., Dunbar, R., and Behrenfeld, M. (2007). Seasonal rhythms of net primary production and particulate organic carbon flux to depth describe the efficiency of biological pump in the global ocean. *J. Geophysical Res.* 112, C10011. doi: 10.1029/2006JC003706
- Matos, F. L., Company, J. B., and Cunha, M. R. (2021). Mediterranean seascape suitability for *Lophelia pertusa*: Living on the edge. *Deep-Sea Res. Part I-Oceanographic Res. Papers* 170. doi: 10.1016/j.dsr.2021.103496
- Mayer, L., Jakobsson, M., Allen, G., Dorschel, B., Falconer, R., Ferrini, V., et al. (2018). The nippon foundation-GEBCO seabed 2030 project: the quest to see the world's oceans completely mapped by 2030. *Geosciences* 8. doi: 10.3390/geosciences8020063
- McCormack, J. E., Zellmer, A. J., and Knowles, L. L. (2010). Does niche divergence accompany allopatric divergence in *Aphelocoma* jays as predicted under ecological speciation? Insights from tests with niche model models. *Evolution* 64, 1231–1244. doi: 10.1111/j.1558-5646.2009.00900.x
- Medina, M., Collins, A. G., Takaoka, T. L., Kuehl, J. V., and Boore, J. L. (2006). Naked corals: Skeleton loss in Scleractinia. *Proc. Natl. Acad. Sci. United States America* 103, 9096–9100. doi: 10.1073/pnas.0602444103
- Morato, T., Gonzalez-Irusta, J.-M., Dominguez-Carriro, C., Wei, C.-L., Davies, A., Sweetman, A. K., et al. (2020). Climate-induced changes in the suitable habitat of cold-water corals and commercially important deep-sea fishes in the North Atlantic. *Global Change Biol.* 26, 2181–2202. doi: 10.1111/gcb.14996
- Mortensen, P. B., and Buhl-Mortensen, L. (2005). "Deep-water corals and their habitats in The Gully, a submarine canyon off Atlantic Canada," in *Cold-water corals and ecosystems*. Eds. A. Freiwald and J. M. Roberts (Springer Berlin Heidelberg, Berlin), 247–277.
- Mortensen, P. B., Buhl-Mortensen, L., Gebruk, A. V., and Krylova, E. M. (2008). Occurrence of deep-water corals on the Mid-Atlantic Ridge based on MAR-ECO data. *Deep-Sea Res. Part II-Topical Stud. Oceanography* 55, 142–152. doi: 10.1016/j.dsr2.2007.09.018
- Overland, J. E., Wang, M., and Box, J. E. (2019). An integrated index of recent pan-Arctic climate change. *Environ. Res. Lett.* 14. doi: 10.1088/1748-9326/aaf665
- Penney, A. J., and Guinotte, J. M. (2013). Evaluation of New Zealand's high-seas bottom trawl closures using predictive habitat models and quantitative risk assessment. *PLoS One* 8. doi: 10.1371/journal.pone.0082273
- Phillips, S. J., Dudik, M., Elith, J., Graham, C. H., Lehmann, A., Leathwick, J., et al. (2009). Sample selection bias and presence-only distribution models: implications for background and pseudo-absence data. *Ecol. Appl.* 19, 181–197. doi: 10.1890/07-2153.1
- Ploton, P., Mortier, F., Rejou-Mechain, M., Barbier, N., Picard, N., Rossi, V., et al. (2020). Spatial validation reveals poor predictive performance of large-scale ecological mapping models. *Nat. Commun.* 11. doi: 10.1038/s41467-020-18321-y

- Portillo-Ramos, R. D. C., Titschack, J., Wienberg, C., Rojas, M. G. S., Yokoyama, Y., and Hebbeln, D. (2022). Major environmental drivers determining life and death of cold-water corals through time. *PLoS Biol.* 20. doi: 10.1371/journal.pbio.3001628
- Price, D. M., Lim, A., Callaway, A., Eichhorn, M. P., Wheeler, A. J., Lo Iacono, C., et al. (2021). Fine-scale heterogeneity of a cold-water coral reef and its influence on the distribution of associated taxa. *Front. Mar. Sci.* 8. doi: 10.3389/fmars.2021.556313
- Ramirez-Llodra, E., Brandt, A., Danovaro, R., De Mol, B., Escobar, E., German, C. R., et al. (2010). Deep, diverse and definitely different: unique attributes of the world's largest ecosystem. *Biogeosciences* 7, 2851–2899. doi: 10.5194/bg-7-2851-2010
- Reed, J. K. (2002). Deep-water *Oculina* coral reefs of Florida: biology, impacts, and management. *Hydrobiologia* 471, 43–55. doi: 10.1023/a:1016588901551
- Rengstorf, A. M., Mohn, C., Brown, C., Wisz, M. S., and Grehan, A. J. (2012). Predicting the distribution of deep-sea vulnerable marine ecosystems using high-resolution data: Considerations and novel approaches. *Deep-Sea Res. Part I: Oceanographic Res. Papers* 93, 72–82. doi: 10.1016/j.dsr.2014.07.007
- Rengstorf, A. M., Yesson, C., Brown, C., and Grehan, A. J. (2013). High-resolution habitat suitability modelling can improve conservation of vulnerable marine ecosystems in the deep sea. *J. Biogeography* 40, 1702–1714. doi: 10.1111/jbi.12123
- Ridgeway, G. (1999). The state of boosting. *Computing Sci. Stat* 31, 172–181.
- Robert, K., Jones, D. O. B., Georgiopolou, A., and Huvenne, V. A. I. (2019). Cold-water coral assemblages on vertical walls from the Northeast Atlantic. *Diversity Distributions* 26, 284–298. doi: 10.1111/ddi.13011
- Robert, K., Jones, D. O. B., Roberts, J. M., and Huvenne, V. A. I. (2016). Improving predictive mapping of deep-water habitats: Considering multiple model outputs and ensemble techniques. *Deep-Sea Res. Part I: Oceanographic Res. Papers* 113, 80–89. doi: 10.1016/j.dsr.2016.04.008
- Roberts, D. R., Bahn, V., Ciuti, S., Boyce, M. S., Elith, J., Guisera-Arroita, G., et al. (2017). Cross-validation strategies for data with temporal, spatial, hierarchical, or phylogenetic structure. *Ecography* 40, 913–929. doi: 10.1111/ecog.02881
- Roberts, J., Wheeler, A., and Freiwald, A. (2006). Reefs of the deep: the biology and geology of cold-water coral ecosystems. *Science* 312, 543–547. doi: 10.1126/science.1119861
- Rodriguez-Galiano, V., Sanchez-Castillo, M., Chica-Olmo, M., and Chica-Rivas, M. (2015). Machine learning predictive models for mineral prospectivity: An evaluation of neural networks, random forest, regression trees and support vector machines. *Ore Geology Rev.* 71, 804–818. doi: 10.1016/j.oregeorev.2015.01.001
- Ross, R. E., and Howell, K. L. (2013). Use of predictive habitat modelling to assess the distribution and extent of the current protection of 'listed' deep-sea habitats. *Diversity Distributions* 19, 433–445. doi: 10.1111/ddi.12010
- Rowden, A. A., Anderson, O. F., Georgian, S. E., Bowden, D. A., Clark, M. R., Pallentin, A., et al. (2017). High-resolution habitat suitability models for the conservation and management of vulnerable marine ecosystems on the louisville seamount chain, south pacific ocean. *Front. Mar. Sci.* 4. doi: 10.3389/fmars.2017.00335
- Rowden, A., Stephenson, F., Clark, M., Anderson, O., Guinotte, J., Baird, S., et al. (2019). Examining the utility of a decision-support tool to develop spatial management options for the protection of vulnerable marine ecosystems on the high seas around New Zealand. *Ocean Coast. Manage.* 170, 1–16. doi: 10.1016/j.ocecoaman.2018.12.033
- Saeedi, H., Warren, D., and Brandt, A. (2022). The environmental drivers of benthic fauna diversity and community composition. *Front. Mar. Sci.* 9. doi: 10.3389/fmars.2022.804019
- Saucier, E. H., Sajjadi, A., and France, S. C. (2017). A taxonomic review of the genus *Acanella* (Cnidaria: Octocorallia: Isididae) in the North Atlantic Ocean, with descriptions of two new species. *Zootaxa* 4323, 359–390. doi: 10.11646/zootaxa.4323.3.2
- Schlitzer, R. (2023). *Ocean data view*. Available at: <https://Http://odv.awi.de>.
- Schoener, T. (1970). Non-synchronous spatial overlap of lizards in patchy habitats. *Ecology* 51, 408–418. doi: 10.2307/1935376
- Sillero, N., and Barbosa, A. M. (2021). Common mistakes in ecological niche models. *Int. J. Geographical Inf. Sci.* 35, 213–226. doi: 10.1080/13658816.2020.1798968
- Slatyer, R. A., Hirst, M., and Sexton, J. P. (2013). Niche breadth predicts geographical range size: a general ecological pattern. *Ecol. Lett.* 16, 1104–1114. doi: 10.1111/ele.12140
- Soetaert, K., Mohn, C., Rengstorf, A., Grehan, A., and van Oevelen, D. (2016). Ecosystem engineering creates a direct nutritional link between 600-m deep cold-water coral mounds and surface productivity. *Sci. Rep.* 6. doi: 10.1038/srep35057
- Stephenson, F., Bowden, D., Finucci, B., Anderson, O., and Rowden, A. (2021a). Developing updated predictive models for benthic taxa and communities across Chatham Rise and Campbell Plateau using photographic survey data. *Fisheries New Z.*
- Stephenson, F., Rowden, A. A., Anderson, O. F., Pitcher, C. R., Pinkerton, M. H., Petersen, G., et al. (2021b). Presence-only habitat suitability models for vulnerable marine ecosystem indicator taxa in the South Pacific have reached their predictive limit. *Ices J. Mar. Sci.* 78, 2830–2843. doi: 10.1093/icesjms/fsab162
- Sundahl, H., Buhl-Mortensen, P., and Buhl-Mortensen, L. (2020). Distribution and Suitable Habitat of the Cold-Water Corals *Lophelia pertusa*, *Paragorgia arborea*, and *Primnoa resedaeformis* on the Norwegian Continental Shelf. *Front. Mar. Sci.* 7. doi: 10.3389/fmars.2020.00213
- Thuiller, W., Georges, D., Gueguen, M., Engler, R., Breiner, F., Lafourcade, B., et al. (2022). *biomod2: Ensemble Platform for Species Distribution Modeling*. R package version 42-1. Available at: <https://cranr-projector/web/packages/biomod2/indexhtml>.
- Tittensor, D. P., Baco, A. R., Brewin, P. E., Clark, M. R., Consalvey, M., Hall-Spencer, J., et al. (2009). Predicting global habitat suitability for stony corals on seamounts. *J. Biogeography* 36, 1111–1128. doi: 10.1111/j.1365-2699.2008.02062.x
- Tong, R., Davies, A. J., Purser, A., Liu, X., and Liu, F. (2022). "Global distribution of the cold-water coral *Lophelia pertusa*," in *IOP Conference Series: Earth and Environmental Science* (Bristol :IOP Publishing). 1004. doi: 10.1088/1755-1315/1004/1/012010
- Tong, R., Purser, A., Guinan, J., Unnithan, V., Yu, J., and Zhang, C. (2016). Quantifying relationships between abundances of cold-water coral *Lophelia pertusa* and terrain features: A case study on the Norwegian margin. *Continental Shelf Res.* 116, 13–26. doi: 10.1016/j.csr.2016.01.012
- Tong, R., Purser, A., Unnithan, V., and Guinan, J. (2012). Multivariate statistical analysis of distribution of deep-water gorgonian corals in relation to seabed topography on the norwegian margin. *PLoS One* 7. doi: 10.1371/journal.pone.0043534
- Tracey, D. M., Rowden, A. A., Mackay, K. A., and Compton, T. (2011). Habitat-forming cold-water corals show affinity for seamounts in the New Zealand region. *Mar. Ecol. Prog. Ser.* 430, 1–22. doi: 10.3354/meps09164
- United Nations. (2015). *Transforming our world: the 2030 Agenda for Sustainable Development*. (A/RES/70/1). Available at: <https://sdgs.un.org/2030agenda>.
- Valavi, R., Elith, J., Lahoz-Monfort, J. J., and Guisera-Arroita, G. (2019). blockCV: An R package for generating spatially or environmentally separated folds for k-fold cross-validation of species distribution models. *Methods Ecol. Evol.* 10, 225–232. doi: 10.1111/2041-210x.13107
- Valavi, R., Elith, J., Lahoz-Monfort, J. J., and Guisera-Arroita, G. (2023). Flexible species distribution modelling methods perform well on spatially separated testing data. *Global Ecol. Biogeography* 32, 369–383. doi: 10.1111/geb.13639
- Valavi, R., Guisera-Arroita, G., Lahoz-Monfort, J. J., and Elith, J. (2022). Predictive performance of presence-only species distribution models: a benchmark study with reproducible code. *Ecol. Monogr.* 92. doi: 10.1002/ecm.1486
- van Oevelen, D., Mueller, C. E., Lundalv, T., and Middelburg, J. J. (2016). Food selectivity and processing by the cold-water coral *Lophelia pertusa*. *Biogeosciences* 13, 5789–5798. doi: 10.5194/bg-13-5789-2016
- Virtanen, P., Gommers, R., Oliphant, T. E., Haberland, M., Reddy, T., Cournapeau, D., et al. (2020). SciPy 1.0: fundamental algorithms for scientific computing in Python. *Nat. Methods* 17, 261–272. doi: 10.1038/s41592-019-0686-2
- Wadoux, A. M.-C., Heuvelink, G. B., De Bruin, S., and Brus, D. J. (2021). Spatial cross-validation is not the right way to evaluate map accuracy. *Ecol. Model.* 457, 109692. doi: 10.1016/j.ecolmodel.2021.109692
- Warren, D. L., Glor, R. E., and Turelli, M. (2008). Environmental niche equivalency versus conservatism: quantitative approaches to niche evolution. *Evolution* 62, 2868–2883. doi: 10.1111/j.1558-5646.2008.00482.x
- Wei, C.-L. (2022). *Data from: chihlinwei/SCC26* (Zenodo). doi: 10.5281/zenodo.6359164
- Wilson, M. F. J., O'Connell, B., Brown, C., Guinan, J. C., and Grehan, A. J. (2007). Multiscale terrain analysis of multibeam bathymetry data for habitat mapping on the continental slope. *Mar. Geodesy* 30, 3–35. doi: 10.1080/01490410701295962
- Winship, A. J., Thorson, J. T., Clarke, M. E., Coleman, H. M., Costa, B., Georgian, S. E., et al. (2020). Good practices for species distribution modeling of deep-sea corals and sponges for resource management: data collection, analysis, validation, and communication. *Front. Mar. Sci.* 7. doi: 10.3389/fmars.2020.00303
- Wolff, A. C., Snaith, H., Amirebrahimi, S., Devey, C. W., Dorschel, B., Ferrini, V., et al. (2019). Seafloor mapping - the challenge of a truly global ocean bathymetry. *Front. Mar. Sci.* 6. doi: 10.3389/fmars.2019.00283
- Yesson, C., Bedford, F., Rogers, A. D., and Taylor, M. L. (2017). The global distribution of deep-water Antipatharia habitat. *Deep-Sea Res. Part II: Topical Stud. Oceanography* 145, 79–86. doi: 10.1016/j.dsr2.2015.12.004
- Yesson, C., Bush, L. E., Davies, A. J., Maggs, C. A., and Brodie, J. (2015). The distribution and environmental requirements of large brown seaweeds in the British Isles. *J. Mar. Biol. Assoc. United Kingdom* 95, 669–680. doi: 10.1017/S0025315414001453
- Yesson, C., Le Te Ssier, T., Nimmo-Smith, A., Hosegood, P., and Proud, R. (2021). Improved bathymetry leads to 4000 new seamount predictions in the global ocean. *UCL Open: Environ.* doi: 10.14324/111.444/ucloe.000030
- Yesson, C., Taylor, M. L., Tittensor, D. P., Davies, A. J., Guinotte, J., Baco, A., et al. (2012). Global habitat suitability of cold-water octocorals. *J. Biogeography* 39, 1278–1292. doi: 10.1111/j.1365-2699.2011.02681.x
- Zhu, G., Li, H., Zhao, L., Man, L., and Liu, Q. (2016). Mapping the ecological dimensions and potential distributions of endangered relic shrubs in western Ordos biodiversity center. *Sci. Rep.* 6. doi: 10.1038/srep26268
- Zweng, M. M., Reagan, J. R., Seidov, D., Boyer, T. P., Locarnini, R. A., Garcia, H. E., et al. (2018). *World ocean atlas 2018, volume 2: salinity* (Mishonov, A. Technical Editor), 40. NOAA Atlas NESDIS 82, Silver Spring.